CENTRO DE INVESTIGACIÓN Y DE ESTUDIOS AVANZADOS DEL INSTITUTO POLITÉCNICO NACIONAL
Unidad Mérida

DEPARTAMENTO DE FÍSICA APLICADA

Descripción de eventos astronómicos en objetos BL Lac y en explosiónes de rayos gamma en un modelo fotohadrónico

TESIS

Que presenta

M. en C. Benjamín Medina Carrillo

Para obtener el grado de

Doctor en Ciencias

en la especialidad de

Física Teórica

Director de Tesis

Dr. Gabriel Sánchez Colón

Co-Director de Tesis

Dr. Sarira Sahu

Mérida, Yucatán, México. Febrero de 2024

CENTRO DE INVESTIGACIÓN Y DE ESTUDIOS AVANZADOS DEL INSTITUTO POLITÉCNICO NACIONAL
Unidad Mérida

APPLIED PHYSICS DEPARTMENT

Description of astronomical events in BL Lac objects and Gamma Ray Bursts in a photohadronic model

THESIS

Presented by

M.Sc. Benjamín Medina Carrillo

To obtain the degree of

Doctor of Science

in

Theoretical Physics

Thesis director

Dr. Gabriel Sánchez Colón

Thesis co-director

Dr. Sarira Sahu

Mérida, Yucatán, México. February 2024

Dedication

With great affection and support from my grandparents Mr. Gustavo and Mrs. Socorro, my dream became a reality.

Acknowledgments

This stage of my life would not have been possible without the support of many people, very precious to me, who deserve to be recognized; therefore, I extend my gratitude:

To my grandparents Mr. Gustavo and Mrs. Socorro, as well as to my mother Carmen Hilda, for the advice, guidance, affection and love that I have received from them, thanks to this, today I conclude one more stage in my academic life.

To all the family members who understood and advised me during this stage of my life.

To my thesis director, Dr. Gabriel Sánchez Colón, for all his teachings, patience and constant advice during my PhD studies and during the realization of this thesis.

To my Co-director of the thesis Dr. Sarira Sahu, for accepting to work with me and who laid the foundation for this doctoral work and the publications we have produced. Thank you for sharing your knowledge at the weekly meetings.

To Dr. Subhash Rajpoot for the contributions, suggestions and corrections made during the work published during the collaboration.

To the Physics Engineer Abigail Valadez Polanco, for her constant support in learning the tools for the development of the research during my first months in the collaboration.

To my partner and friend Diana Páez, student at the Faculty of Sciences of the UNAM, for the great support during the research we have carried out together during the collaboration with the aforementioned Drs.

To Drs. Cristina Vargas, José Mustre, Antonio Bouzas and Francisco Larios, for accepting to be part of the synods. For their corrections and recommendations for this thesis.

To Zhirnay Rodríguez for her secretarial support and in general to all the administrative staff of the Applied Physics Department of the Cinvestav-IPN Mérida Unit for all the attention given to me during my PhD studies.

To my friends Juan Pablo and Luis Jiménez, who are currently in the final stage of their PhD. studies in this Unit, I thank you for all your advice and healthy coexistence.

To my good friend Daniel Aké, for all the coexistence we have had since our studies in the master's program and for the advice that has helped me in other areas of my life.

To my other classmates and friends that I have forged during my studies at CINVESTAV, for creating a pleasant environment during my studies.

To Engineer Ángel Koyoc, a very dear friend who during the last 15 years, besides instructing me in the discipline of "banda de guerra", has advised me in various areas of life to be a better person in life.

To my dear friends Vanesa, Trinidad, Carolina, Reyna, Christopher and Russell; may we never lack those moments of healthy fellowship. Thank you for being a big part of my life.

To all those friends who have been there at some point in my life.

To DGAPA-UNAM (México) Project No. IN103522 and California State University-Long Beach for support the research projects published during the collaboration.

To CONAHCyT for its financial support during the years of doctoral studies.

Abstract

Very high-energy (VHE) flaring events that occurred in the BL Lac objects PGC 2402248 and VER J0521+211, were observed using the Very Energetic Radiation Imaging Telescope Array System (VERITAS) and Major Atmospheric Gamma Imaging Cherenkov (MAGIC) telescopes. Additionally, an exceptionally intense gamma-ray burst (GRB), GRB 221009A, was detected on 2022 October 9, by multiple instruments. A photohadronic model is employeded to describe the VHE events observed in PGC 2402248, in order to compare the results with those obtained from other emission models. It is found that the photohadronic fits to PGC 2402248 observations are comparable and even far better than the obtained with most other models. Additionally, for the analysis of the VHE spectra of VER J0521+211, three different extragalactic background light (EBL) models are employed to determine constraints on its redshift (z). The analysis shows that, the photohadronic model, coupled with the EBL model proposed by Dominguez et al. 2011, imposes the most constraining limits on z. Finally, a scenario is proposed to show that the VHE photons from GRB 221009A can be observed on the Earth from the interaction of VHE protons with the seed synchrotron photons in the external forward shock region of the GRB jet.

Resumen

Los eventos de llamaradas de muy alta energía (VHE) que tuvieron lugar en los objetos BL Lac PGC 2402248 y VER J0521+211, fueron observados utilizando los telescopios Very Energetic Radiation Imaging Telescope Array System (VERITAS) y Major Atmospheric Gamma Imaging Cherenkov (MAGIC). Además, un estallido de rayos gamma (GRB) excepcionalmente intenso, GRB 221009A, fue detectado el 9 de octubre de 2022 por múltiples instrumentos. Se utiliza un modelo fotohadrónico para describir los eventos VHE observados en PGC 2402248, a fin de comparar los resultados con los obtenidos a partir de otros modelos de emisión. Se encuentra que los ajustes fotohadrónicos a las observaciones de PGC 2402248 son comparables e incluso mucho mejores que los obtenidos con la mayoría de los otros modelos. Además, para el análisis de los espectros VHE de VER J0521+211, se emplean tres modelos diferentes de luz de fondo extragaláctica (EBL) para determinar restricciones sobre su desplazamiento al rojo (z). El análisis muestra qué, el modelo fotohadrónico acoplado con el modelo EBL propuesto por Domínguez et al. 2011, impone los límites más restrictivos a z. Por último, se propone un escenario que muestra que los fotones VHE del GRB 221009A pueden observarse en la Tierra a partir de la interacción de protones VHE con los fotones sincrotrón semilla en la región de choque frontal externo del chorro del GRB.

Contents

List of Figures

List of Tables

Introduction

Blazars are a subclass of active galactic nuclei (AGN) that are known to be the dominant extragalactic population in γ-rays (V. A. Acciari et al. 2011). These objects exhibit rapid variability in their emission across the entire electromagnetic spectrum, from radio waves to γ-rays. The spectra of a BL Lac object, a subclass of blazars, are characterized by their non-thermal emission, which overwhelms the contribution from the stellar emission of the host galaxy. This dominance of non-thermal emission can make it challenging to estimate the redshift of the source. The redshift of a BL Lac object is a crucial parameter as it provides important information about the intrinsic spectrum, the nature of the source, and its cosmological evolution. On the other hand, that the spectral emission is non-thermal suggests that the observed photons originate within highly relativistic jets that are oriented very close to the line of sight of the observer (Urry and Paolo Padovani 1995). The small viewing angle of the jet in blazars allows us to observe strong relativistic effects: firstly, the relativistic boosting of the emitted power, and secondly, a shortening of the characteristic time scales, as short as minutes or even seconds (F. Aharonian et al. 2007; Abdo, Ackermann, Ajello, Atwood, Axelsson, et al. 2009). Thus, these objects are important for studying the energy emission mechanisms from the central supermassive black hole, the physical properties of the astrophysical jets, and the production of ultra-high energy cosmic rays, very high energy (VHE) γ-rays and neutrinos.

The spectral energy distribution (SED) of blazars typically exhibits a distinctive double-peak structure in the frequency versus flux ($\nu - \nu F_\nu$) plane (Abdo, Ackermann, Agudo, et al. 2010). The general consensus is that the low-energy peak originates from the synchrotron emission of accelerated electrons and positrons in the magnetic field of the blazar jet. The high-energy peak of the SED, on the other hand, can be produced through two main mechanisms. One possibility is synchrotron self-Compton (SSC)

scattering, where the high-energy electrons in the jet interact with the synchrotron photons they themselves produce (L. Maraschi, G. Ghisellini, and Celotti 1992; Murase et al. 2012; Gao et al. 2013). Another possibility is the up-scattering of low-energy external seed photons by ultra-relativistic electrons in the jet. The sources of these seed photons can be various regions surrounding the central supermassive black hole, such as the accretion disk, the broad line regions, or the dusty torus (Dermer and Schlickeiser 1993; Sikora, Begelman, and Rees 1994; Błażejowski et al. 2000). In both cases, the energy of the low-energy photons are increased by collisions with the high-energy electrons. Alternatively, the origin of the high-energy peak in the SED can involve a combination of leptonic and hadronic processes occurring within the blazar jet and its surrounding environment (Matteo Cerruti 2020). According to the position of the synchrotron peak frequency, the BL Lac objects are usually classified as follows, low-energy peaked blazars (LBLs, $\nu_{peak} < 10^{14}$ Hz), intermediate-energy peaked blazars (IBLs, 10^{14} Hz $< \nu_{peak} < 10^{15}$ Hz), high-energy peaked blazars (HBLs, 10^{15} Hz $< \nu_{peak} < 10^{17}$ Hz) (Paolo Padovani and Giommi 1995; Abdo, Ackermann, Agudo, et al. 2010; M. Böttcher et al. 2013), and extreme high-energy peaked blazars (EHBLs, $\nu_{peak} > 10^{17}$ Hz) (L. Costamante et al. 2001). The leptonic model, which attributes the production of the SED to the interaction of leptons ($e^{\pm}$), has been very successful in explaining the multiwavelength emission from blazars and Fanaroff-Riley Class I galaxies (FR-I) (Fossati et al. 1998; G. Ghisellini, Celotti, et al. 1998; Abdo, Ackermann, Ajello, Atwood, Baldini, et al. 2010; Roustazadeh and M. Böttcher 2011). The inevitable outcome of the leptonic models, flaring at TeV energies should be accompanied by a simultaneous flaring in the synchrotron peak. However, non observation of low energy counterparts have been observed in many flaring blazars, for example, the flares observed from HBL 1ES 1959+650 in 2022 May (Holder et al. 2003; F. Aharonian, Akhperjanian, and Beilicke 2003; Krawczynski et al. 2004), and Markarian 421 in 2004 (Błażejowski. et al. 2005) have presented challenges to pure leptonic models and are in favor of hadronic model or hybrid (hadronic+leptonic) models. It is to be noted that, recent observation of a high-energy neutrino event correlated with a flaring blazar by the IceCube neutrino observatory suggests the involvement of hadronic processes in these astrophysical phenomena (IceCube Collaboration et al. 2018; Ansoldi et al. 2018). For neutrinos to be produced in blazars, VHE protons or nuclei are required, so that their interaction with the surrounding background can produce pions and subsequent decay of pions will produce neutrinos and

γ-rays.

Flaring is the major activity observed in blazars, characterized by unpredictable and rapid changes in their emission states (switches between quiescent and active states). These flaring events can occur on various time scales and exhibit different flux levels. In some blazars, there is a strong temporal correlation between the X-ray and multi-TeV gamma-ray emissions during flaring episodes. However, in some other cases, flaring events lack low-energy counterparts, resulting in what is known as "orphan flaring" (Krawczynski et al. 2004; Błażejowski. et al. 2005). It is also very important to have simultaneous multiwavelength observations during the flaring periods are crucial to better understand the emission mechanisms and to constrain theoretical models in different energy regimes.

Different theoretical models have been proposed to explain the flaring activity in AGNs, and they can be broadly categorized into leptonic models and hadronic models. The leptonic model, which involves the upscattering of low-energy photons by high-energy electrons through the SSC process, has limitations in explaining VHE gamma-ray emission and orphan flaring observed in many blazars. The multi-zone leptonic model is a more sophisticated version of the pure leptonic model that can help explain the high-energy emissions, including VHE gamma-rays and orphan flaring, observed in blazars. In this model, the emission region is divided into multiple zones, each characterized by different physical conditions and parameters. However, it is important to note that increasing the number of parameters in the model also increases the complexity of interpreting the observational data. In the hadronic synchrotron-proton blazar model (F. A. Aharonian 2000; Muecke et al. 2003; Reimer, Protheroe, and Donea 2004), the emission of synchrotron photons from protons take place, these Fermi accelerated protons emit synchrotron radiation as they spiral along the magnetic field lines. However, the synchrotron radiation from protons is expected will be suppressed by a factor of m_p^{-4}, where m_p is the proton mass. Therefore a significant flux of ultra-high-energy protons is required to explain the observed VHE γ-rays. It also needs a strong magnetic field for the synchrotron process to be effective but a strong magnetic field in the jet is not commonly observed in blazars. The jet-in-jet model (proposed by Giannios, Uzdensky, and Begelman 2010) suggests that within the main jet of a blazar, smaller jets or "mini jets"can be formed due to flow instabilities. These mini jets are thought to move relativistically concerning the main jet flow. In this model, the interaction between the daughter mini jets and the main jet is believed

to be responsible for the production of VHE γ-rays. While the mini jets are aligned with our line of sight, the VHE gamma rays are beamed with a large Doppler factor. The lepto-hadronic model (Reynoso, Medina, and Romero 2011) using instruments such as the Large Area Telescope (LAT) and the High-Energy Stereoscopic System (H.E.S.S.), has been successful in fitting the low-energy γ-ray spectrum observed during the low state, but not the flaring state of blazars. Similarly, the magnetosphere model (F. M. Rieger and F. A. Aharonian 2008; Frank M. Rieger and Levinson 2010; Frank M. Rieger 2011) has been proposed as an alternative to explain the hard TeV spectrum from blazars. However in this case, there may be limitations in providing detailed quantitative predictions for the VHE light curves during flaring states. The VHE SEDs of blazars can be modeled using various hadronic models (Rachen 2000; F. A. Aharonian, Timokhin, and Plyasheshnikov 2002; Maria Petropoulou et al. 2017; M. Petropoulou, Nalewajko, et al. 2017). By modeling the hadronic processes in blazars, it becomes possible to estimate the fluxes of high-energy cosmic rays and neutrinos (Halzen and Hooper 2005; Fraija and Marinelli 2016; M. Petropoulou, Coenders, and Dimitrakoudis 2016).

A distinctive feature of the high-energy γ-rays, is that they propagate through the universe, interact with the extragalactic background light (EBL), and undergo energy-dependent attenuation en route to Earth. This attenuation is primarily caused by the process of electron-positron pair production (Stecker, Jager, and Salamon 1992). The interaction with the EBL not only attenuates their flux but also alters the spectral shape of the VHE photons. Understanding the SED of the EBL is crucial for accurately interpreting the deabsorved VHE γ-ray spectra from astrophysical sources. Directly measuring the EBL is challenging due to various factors that introduce uncertainties, one significant challenge is the contribution of zodiacal light (Hauser and Dwek 2001; Chary and Pope 2010), and another challenge is the galaxy counts provide a lower limit since the exact contribution from faint unresolved sources remains uncertain (Madau and Pozzetti 2000). Due to the challenges involved in directly detecting and measuring the EBL contribution, various approaches have been developed to estimate the EBL density as a function of energy for different redshifts through lepton pair production. The observed VHE flux of a blazar F_γ is related to the intrinsic flux $F_{int,\gamma}$ through the relation (Hauser and Dwek 2001)

$$F_\gamma(E_\gamma) = F_{int,\gamma}(E_\gamma)\, e^{-\tau_{\gamma\gamma}(E_\gamma,z)} \tag{1}$$

where the optical depth ($\tau_{\gamma\gamma}$) for the process $\gamma\gamma \rightarrow e^+e^-$ depends on the energy of the γ-ray photons (E_γ) and the redshift (z) of the source. The exponential factor in the equation corresponds to the attenuation or depletion of the VHE γ-ray flux due to the interaction with the EBL and subsequent production of electron-positron pairs. Several EBL models (Franceschini et al. 2008; Finke, Razzaque, and Dermer 2010; Domínguez et al. 2011; Gilmore et al. 2012) have been developed to study the attenuation of high-energy gamma rays at different redshifts.

Another astronomical event of great interest are gamma-ray bursts (GRB). The birth of GRBs is associated with the collapse of massive stars or the merger of compact binary systems. These events lead to the formation of stellar-mass black holes or rapidly rotating neutron stars known as magnetars (Piran 2004; Pawan Kumar and Zhang 2015). In the external shock model, the relativistic ejecta or fireball produced during the prompt phase interacts with the surrounding circumstellar medium. This interaction leads to the development of two shocks. The one that lasts longer is the forward shock is the primary shock that continues to propagate into the surrounding medium, while the reverse shock moves back into the fireball. The synchrotron radiation from these accelerated electrons is believed to be responsible for the γ-ray emission observed above around 100 MeV in the afterglow shocks (Sari and Esin 2001; P. Kumar and Barniol Duran 2009; G. Ghisellini, Ghirlanda, et al. 2010; X.-Y. Wang, He, et al. 2010). However, it becomes challenging to explain the detection of sub-TeV photons at late times (>100 seconds), where the shock has already decelerated substantially. Beyond the synchrotron limit, alternative radiation mechanisms need to be invoked to explain the sub-TeV emission observed (Asano, Inoue, and Mészáros 2009; Razzaque, Dermer, and Finke 2010; Razzaque 2010; Asano and Mészáros 2012). Also, joint observations of X-rays by the Swift X-ray Telescope and gamma rays by the Fermi Large Area Telescope have provided valuable insights into the spectral properties of GRBs. Studies, such as the one conducted by Ajello et al. 2018, have found that can be described by a single spectral component. The synchrotron mechanism has limitations in producing photons above a few GeV without the use of unrealistically large bulk Lorentz factors (Razzaque, Dermer, and Finke 2010). The fireball model predicts that GeV–TeV photons can originate from the GRB fireball and that the emission can persist for minutes to several hours (Piran 2004; Pawan Kumar and Zhang 2015). The SSC process is a favored mechanism for interpreting very high-energy (VHE > 100 GeV) photons in the afterglow

era of GRBs, where the relativistic electrons scatter their synchrotron radiation (Waxman 1997; Sari and Esin 2001; Zhang and Mészáros 2001; Pawan Kumar and Zhang 2015). In the scenario mentioned, the SSC emission can occur either from a constant density circumburst medium or from the Comptonization of X-ray photons in the afterglow shock (Derishev and Piran 2019; X.-Y. Wang, Liu, et al. 2019).

As the leptonic and lepto-hadronic models have limited predictability due to a large number of parameters, here we have a revised look into the hadronic model, particularly the photohadronic one. In a series of papers by Sahu et al., we explore the photohadronic scenario as an explanation for the GeV-TeV flaring observed in many blazars. In this scenario, high-energy protons accelerated by the Fermi mechanism interact with the background photons present in the jet environment. These interactions can lead to the production of Delta resonances (Δ^+), subsequently decay into pions, which in turn can produce VHE γ-rays and neutrinos. The VHE γ-rays are observed and can provide a good fit to the spectra observed during the flaring activity of blazars. The success of the photohadronic model is presented in refs. (Sahu and Fortín 2020; Sahu, Polanco, and Rajpoot 2022), taking into account that there are many similarities between blazar and GRB jets (J. Wang and Wei 2010; Nemmen et al. 2012). In those works, the success of the photohadronic model is once again exploited to explain sub-TeV emissions from GRB objects.

The plan of this work is as follows. In chapter 1, a detail discussion about the photohadronic model and the kinematical condition for the process $p + \gamma \to \Delta^+$ and its subsequent decay is given. Also, the relation between the observed GeV-TeV γ-ray flux and the γ-ray from the photohadronic process is shown. In chapter 2, an analysis was made of the VHE spectrum of the EHBL PGC 2402248 observed by the MAGIC telescopes in the context of the photohadronic model using different EBL models. The results were compared with the other emission models reported in the bibliography, and we observed that our model fits are far better than the ones of the most other models. In chapter 3, the photohadronic model of Sahu 2019 is used with the three well-known EBL models (Franceschini et al. 2008; Domínguez et al. 2011; Gilmore et al. 2012) to analyse the VHE flaring events of 2009-2010 and 2013-2014 observed by VERITAS and MAGIC collaborations and to obtain constraints on the limiting values of the redshift of the IBL VER J0521+211. In chapter 4, the common features of blazars and GRBs are discussed and the afterglow phase of GRB 221009A with the photohadronic

model of Sahu 2019 is studied. Possible explanations are sought, within the physics of the Standard Model, for the ultra-high energy photons, $\sim$18 TeV, detected in the object GRB 221009A by the LHAASO collaboration. Finally, the conclusions about the obtained results are presented.

Chapter 1

Photohadronic Model

1.1 Photohadronic scenario

The photohadronic model is employed to elucidate high-energy γ-ray emissions originating from astronomical sources, particularly blazars. This model is based on the conventional interpretation of the first two peaks in the SED. Specifically, the first peak is due to synchrotron radiation produced by relativistic electrons within the jet environment, while the second peak results from the SSC process (Dermer and Schlickeiser 1993; Sikora, Begelman, and Rees 1994).

This model operates under the assumption of a double jet structure along the common axis (Sahu 2019; Sahu, Fortín, and Nagataki 2019). During VHE flaring events, a compact and confined smaller jet with a size R'_f is formed within a larger jet characterized by a size denoted as R'_b (It is important to note that $R'_f < R'_b$, the primed symbols indicate quantities as measured in the comoving frame of the jet). In this context, it is emphasized that the photon density within the inner jet region, denoted as $n'_{\gamma,f}$, is significantly greater than the photon density in the outer jet region, represented as n'_γ ($n'_\gamma << n'_{\gamma,f}$). As the inner jet expands adiabatically and transitions into the outer region, the photon density is expected to decrease. To account for this change, the assumption of a scaling behavior of the photon densities in both the inner and the outer regions is made. The geometrical description of the jet structure during a flare is illustrated in fig. 1 of Sahu 2019. Although the bulk Lorentz factor of the inner jet, denoted as Γ_{in}, moves (slightly) faster than the bulk Lorentz factor of the outer jet, denoted as Γ_{ext}, their respective

bulk Lorentz factors satisfy $\Gamma_{in} > \Gamma_{ext}$. In this scenario, for simplicity, it is assumed that both the internal and external jets have the same bulk Lorentz factor, $\Gamma_{in} \simeq \Gamma_{ext} \simeq \Gamma$, and that the Doppler factor, represented as $\mathcal{D}$, is approximately equal to the Lorentz factor ($\Gamma \simeq \mathcal{D}$) (G. Ghisellini, Celotti, et al. 1998; Krawczynski et al. 2004).

Within the constrained volume, protons are accelerated to extremely high energies, and their differential spectrum is described by a power law of the form, where the proton energy, denoted as E_p is related to the spectral index, denoted as α, as follows: $dN_p/dE_p \propto E_p^{-\alpha}$ with $\alpha \geq 2$ (Dermer and Schlickeiser 1993; Gupta 2008). However, the value of α can vary depending on the specific type of shock involved (non-relativistic shocks, highly relativistic shocks and oblique relativistic shocks) (Keshet and Waxman 2005; Summerlin and Baring 2012). In the inner jet region, these high-energy protons interact with the SSC background seed photons, resulting in the production of the Δ-resonance ($p + \gamma \rightarrow \Delta^+$), of the form

$$p + \gamma \rightarrow \Delta^+ \rightarrow \begin{cases} p\,\pi^0, & \text{fraction } 2/3 \\ n\,\pi^+, & \text{fraction } 1/3 \end{cases} \tag{1.1}$$

with a cross section $\sigma_\Delta \sim 5 \times 10^{-28}$ cm^2. Within the energy range being examined, both the direct single pion production and the multipion production processes are contributing factors, but are not efficient (Mücke et al. 1999; Owen et al. 2018). We neglect such contributions in this work. Following the production of charged and neutral pions, the charged pions will decay through a process $\pi^+ \rightarrow e^+ \nu_e \nu_\mu \overline{\nu}_\mu$. On the other hand, the neutral pions will decay through $\pi^0 \rightarrow \gamma\gamma$. In this scenario, the γ-rays generated as a result of the decay of neutral pions constitute the VHE γ-rays that are observed on Earth.

1.2 Kinematical condition

Equation 1.1, indicates that the center of mass energy of the interaction must exceed the rest mass energy of the Δ-particle, which is approximately 1.232 GeV, which corresponds to the following kinematic condition

$$E'_p \epsilon'_\gamma = \frac{m^2_{\Delta^+} - m^2_p}{2\,(1 - \beta_p \cos\theta)} \simeq 0.32 \text{ GeV}^2 \tag{1.2}$$

here E'_p represents the energy of a proton in the comoving frame of the jet, and ϵ'_γ represents the energy of a background photon in the same comoving frame. The kinematic condition can be rewrite, in the observer frame, as

$$E_p \epsilon_\gamma \simeq 0.32 \ \frac{\Gamma \mathcal{D}}{(1+z)^2} \mathrm{GeV}^2 \tag{1.3}$$

where

$$\epsilon_\gamma = \frac{\mathcal{D} \epsilon'_\gamma}{(1+z)} \tag{1.4}$$

typically represents the observed energy of background photons, while

$$E_p = \frac{\Gamma E'_p}{(1+z)} \tag{1.5}$$

is the energy of proton, measured by an observer on Earth. This measurement assumes that the proton could escape from its source to Earth without any loss of energy. Additionally, z represents the redshift of the object.

Given that every π^0 particle decays into two γ-rays, the energy (E_γ) of the γ-ray photons resulting from the π^0 decay in the observer's frame can be formulated as follows

$$E_\gamma = \frac{1}{10} \frac{\mathcal{D}}{(1+z)} E'_p = \frac{\mathcal{D}}{10\Gamma} E_p \tag{1.6}$$

To blazars, it is important to recall that $\Gamma \simeq \mathcal{D}$, leading to the relation $E_p = 10 E_\gamma$. Consequently, the kinematical condition between the energy of the π^0 decay photon, E_γ, and the energy of the photon, ϵ_γ, can be expressed as follows

$$E_\gamma \epsilon_\gamma \simeq \frac{0.032 \ \mathcal{D}^2}{(1+z)^2} \ \mathrm{GeV}^2 \tag{1.7}$$

Then, once you have the known flare energy E_γ of a blazar and the $\mathcal{D}$, determined from the leptonic model fitting to the blazar SED, you can calculate the seed photon energy ϵ_γ using the kinematical condition between E_γ and ϵ_γ.

1.3 Flux calculation

Observed VHE γ-ray flux is influenced by two factors: the background seed photon density, and the differential power spectrum of Fermi-accelerated protons, which can be expressed as $F_\gamma \propto n'_\gamma(E_p^2 dN/dE_p)$. To account for the multi-TeV emissions observed during flaring events within the photohadronic scenario, the jet kinetic power must elevate to the super-Eddington limit (G. Cao and Jiancheng Wang 2014; Zdziarski and Markus Böttcher 2015). However, due to the higher photon density, the inner compact jet scenario evades this problem (Sahu, Oliveros, and Sanabria 2013). The optical depth of the Δ-resonance process in the inner jet region can be expressed as follows

$$\tau_{p\gamma} = n'_{\gamma,f}\sigma_\Delta R'_f \tag{1.8}$$

Assuming that the Eddington luminosity L_{Edd} is equally shared between the jet and the counter jet during a flaring event, the luminosity L'_{jet} for a seed photon of energy ϵ'_γ satisfies the condition $L'_{jet} \ll L_{Edd}/2$. This condition implies the following

$$\tau_{p\gamma} \ll \frac{L_{Edd}}{8\pi}\frac{\sigma_\Delta}{R'_f\,\epsilon'_\gamma} \tag{1.9}$$

Since the inner jet region is obscured from direct observation, it is challenging to determine the photon density within that region directly. However, due to the adiabatic expansion of the inner jet as it transitions into the outer jet, the photon density decreases to a value represented as n'_γ. This reduction in photon density results in the suppression of the efficiency of the process $p + \gamma \to \Delta^+$, leading to an optical depth $\tau_{p\gamma} \ll 1$. This is the reason why, in a single jet scenario, the efficiency of Δ-resonance production is suppressed, and to account for the observed VHE γ-ray flux within the hadronic model, it is necessary to have a super-Eddington luminosity in protons. However, the presence of the additional compact inner jet in our scenario addresses the challenge of the excess energy budget required in protons (Sahu, León, and Miranda 2017). From the SED data, it is possible to calculate the photon density in the outer jet region, denoted as n'_γ. For the sake of simplicity, we assume that the photon densities in both the inner and outer jet regions exhibit a scaling behavior, which can be represented as follows (Sahu 2019; Sahu, Fortín, and Nagataki 2019)

$$\frac{n'_{\gamma,f}(\epsilon_{\gamma,1})}{n'_{\gamma,f}(\epsilon_{\gamma,2})} \simeq \frac{n'_\gamma(\epsilon_{\gamma,1})}{n'_\gamma(\epsilon_{\gamma,2})} \tag{1.10}$$

In the equation provided, the left-hand side represents the unknown photon density in the inner region, while the right-hand side contains known values. This equation serves to express the unknown photon density in the inner region in terms of the known photon density in the outer region. In the outer region, the phonton density can be determined in terms of the SSC photon energy and its corresponding flux $\Phi_{SSC}(\epsilon_\gamma)$ of the form, $n'_\gamma(\epsilon_\gamma) \propto \Phi_{SSC}(\epsilon_\gamma)\epsilon_\gamma^{-1}$. Then, using the equation 1.10 we can express $n'_{\gamma,f}$ in terms of Φ_{SSC}. In numerous prior studies, it has been demonstrated that the Φ_{SSC} in the low-energy tail region exhibits a perfect power-law behavior for HBLs, and for many persistently active EHBLs, this flux can be represented as $\Phi_{SSC} \propto \epsilon_\gamma^\beta \propto E_\gamma^{-\beta}$ with $\beta > 0$ (Sahu 2019; Sahu, Fortín, and Nagataki 2019). The observed VHE γ-ray flux, denoted as F_γ, depends on both the seed photon density, $n'_{\gamma,f}$, and the high-energy proton flux, represented as F_p and defined as $F_p \equiv E_p^2 dN/dE_p$. When we express $n'_{\gamma,f}$ in terms of Φ_{SSC}, it leads to the relationship that F_γ is proportional to $n'_{\gamma,f}$ and can be expressed as $F_\gamma \propto n'_{\gamma,f} \propto E_\gamma^{-\beta+1}$. Analogously, for $F_\gamma \propto F_p$, we deduce $F_\gamma \propto E_\gamma^{-\alpha+2}$. The VHE γ-ray flux experiences attenuation due to the EBL effect, which is quantified by a factor $e^{-\tau_{\gamma\gamma}}$ (Stecker, Jager, and Salamon 1992; Ackermann et al. 2012; P. Padovani et al. 2017). Here, $\tau_{\gamma\gamma}$ represents the optical depth associated with the process of lepton pair production, $\gamma\gamma \to e^+e^-$, and depends on the z and E_γ. Considering the EBL correction, the observed VHE flux of γ-rays on Earth is (comparing with Eq. 1)

$$F_\gamma(E_\gamma) = F_{\gamma,int}(E_\gamma)\, e^{-\tau_{\gamma\gamma}(E_\gamma,z)} = F_0 \left(\frac{E_\gamma}{TeV}\right)^{-\delta+3} e^{-\tau_{\gamma\gamma}(E_\gamma,z)} \tag{1.11}$$

here, the parameter δ is defined as the sum of α and β, which falls within the range of $2.5 \leq \delta \leq 3.0$, as indicated by Sahu 2019, and the work by Sahu, Fortín, and Nagataki 2019. F_0 is the normalization constant, and it is typically determined from the observed VHE spectrum. On the other hand, $F_{\gamma,int}$ represents the intrinsic VHE flux.

In the photohadronic process, where each pion carries approximately 20% of the proton energy and each neutrino produced from the decay of a positively charged pion (π^+) carries about 25% of the pion energy, and this given the relationship $E_\nu = E_\gamma/2$. The neutrino flux, F_ν, can be calculated from F_γ, of the form (Sahu, Oliveros, and Sanabria 2013)

$$F_\nu = \frac{3}{8} F_\gamma \tag{1.12}$$

It is crucial to emphasize that the photohadronic process is particularly effective for E_γ greater than or approximately equal to 100 GeV. Below this energy threshold, other processes, particularly leptonic mechanisms such as the electron synchrotron mechanism and the SSC process, tend to have the dominant contribution to the multiwavelength SED.

Chapter 2

Emission mechanism in the EHBL PGC 2402248

For the first time, MAGIC telescopes detected multi-TeV γ-rays from the EHBL PGC 2402248 on 2018 April 19, several instruments observed the γ-rays flux of the source in multiwavelength. Broad-band SED of the source is modeled using both leptonic and hadronic models. Extending the success of the photohadronic model to explain the VHE events from PGC 2402248 observed by MAGIC telescopes to compare our results with other models. We observed that the fits obtained with the photohadronic model are comparable and even fare better than most other models. Additionally, we show that the spectrum is in a low-emission state and is not hard. The estimated bulk Lorentz factor for this flaring event is $\lesssim 34$.

2.1 Flaring of PGC 2402248

MAGIC collaboration conducted an observational program with the specific goal of discovering new EHBLs. The selection of the object PGC 2402248 (also identified as 2WHSP J073326.7+515354) from the 2WHSP catalogue (as published by Chang et al. 2017) was based on a specific parameter: its high synchrotron peak frequency, denoted as ν_{syn}^{peak}, which was measured to be approximately $10^{17.9}$ Hz. Between the dates of 2018 January 23 and April 19 (which corresponds to MJD 58141 - MJD 58227), MAGIC telescopes conducted observations of the source during 25 nights for a total of 23.4 h. On April 19, for the first time, the telescopes detected TeV γ-rays originating

from the blazar PGC 2402248. In this observational period of the MAGIC telescopes, simultaneous multiwavelength observations were conducted by the Swift-UVOT and the KVA in the ultraviolet and optical bands, in the X-ray band by the Swift-XRT, and in the γ-ray band by the Fermi-LAT (Acciari et al. 2019). As part of the observational campaign to characterize the source, additional observations were conducted using the Gran Telescopio Canarias (GTC) optical telescope. These observations aimed to determine the z of the source, which was previously unknown. The results of these observations, as reported by Becerra Gonzalez et al. 2018, revealed that the redshift of PGC 2402248 is $z = 0.065$. The study of the broad-band SED of PGC 2402248 involved the incorporation of γ-ray archival data obtained over a substantial period exceeding 10 years. Specifically, the data was collected from 2008 August 4 to 2019 June 24, by Fermi-LAT instrument to construct the multiwavelength SED and to examine the flux variability. The estimate of the synchrotron peak frequency was through a combination of data sources and simultaneous observations of the Swift-XRT and the MAGIC telescopes, and 105-month non-simultaneous archival data obtained from Swift-BAT. The resulting estimate was $\nu_{syn}^{peak} = 10^{17.8\pm0.3}$ Hz, this estimate was consistent with the value documented in the 2WHSP catalogue. The consistent estimate of the ν_{syn}^{peak} during various observation periods, suggests that PGC 2402248 can be classified as a stationary EHBL. During the observational period conducted by the MAGIC telescopes on PGC 2402248, the simultaneous observations revealed that there was no significant variability in the gamma-ray emissions from the source. However, there was moderate variability observed in the Swift-UVOT and Swift-XRT data. Fitting the spectrum of long-term observations has the potential to average out the short-term variability that may be present in the data. While the overall non-variability in the SED during the MAGIC observations on PGC 2402248 indicates that the source was in a stable state over the long-term observational period, the presence of short-term flaring events cannot be ignored.

2.2 Results and analysis

Concurrent multiwavelength observations of the blazar PGC 2402248 during the MAGIC observation period from 2018 January 23 to April 19, combined with 10 years of archival data collected by the Fermi-LATtelescope, were instrumental in constructing the broad-band SED of this source with a

Table 2.1: VHE spectrum in Fig. 2.4 and the broad-band SED of PGC 2402248 in Fig. 2.5, are fitted with several different models: the one-zone SSC, the 1D conical jet, the spine-layer, the proton-synchrotron, and the photohadronic. Bulk Lorentz factor (Γ), the magnetic field (B' in G), and the blob radius (R'_b in 10^{16} cm; Acciari et al. 2019), used in these fits, are shown.

Model	Γ	R'_b	B'
One-zone SSC	30	1	0.01
1D conical jet	30	2.1	0.005
Spine-layer	30, 5	3, 3.5	0.02, 0.1
Proton-synchrotron	30	0.1–14.6	1.2–46.8
Photohadronic	≤ 34	1	$\sim 10^{-4.3}$

high degree of precision. This data analysis was reported in the publication by Acciari et al. 2019. In this work, the X-ray data have provided information indicating that the synchrotron peak frequency of the source is located in the EHBL region. Furthermore, the observed VHE γ-ray spectrum, which has been reconstructed in the energy range from 0.1 to 8 TeV, is well-described by a power-law spectrum, that is given by the equation: $dN/dE_\gamma = f_0(E_\gamma/200\ \mathrm{GeV})^{-\lambda}$, where $f_0 = (1.95 \pm 0.10_{stat}) \times 10^{-11}$ph cm^{-2} s^{-1} TeV^{-1}, and $\lambda = 2.41 \pm 0.17_{stat}$, and the intrinsic spectrum, as shown in Figure 2 of the same reference, is well-described by a power-law that remains nearly flat in the energy regime considered. Additionally, in the work of Acciari et al. 2019, various models were employed to fit the multiwavelength SED of the source. These models include the proton-synchrotron model (M. Cerruti et al. 2015), the 1D conical jet model (Asano and Hayashida 2015; Asano and Hayashida 2018), the spine-layer model (G. Ghisellini, F. Tavecchio, and Chiaberge 2005), and the one-zone SSC model (L. Maraschi, G. Ghisellini, and Celotti 1992; Fabrizio Tavecchio, Laura Maraschi, and Gabriele Ghisellini 1998). The conclusion in this report was that extreme physical parameters are required for three out of the four SED modeling scenarios suggesting that these models may not be consistent with the observed data. On the other hand, the spine-layer model appears to be the most promising and reasonable framework for explaining the broad-band SED of PGC 2402248.

In this part of the project, we employed a photohadronic model, as described in Eq. 1.11, along with the EBL model proposed by Franceschini et al. 2008 to successfully fit the VHE γ-ray spectrum that had been observed

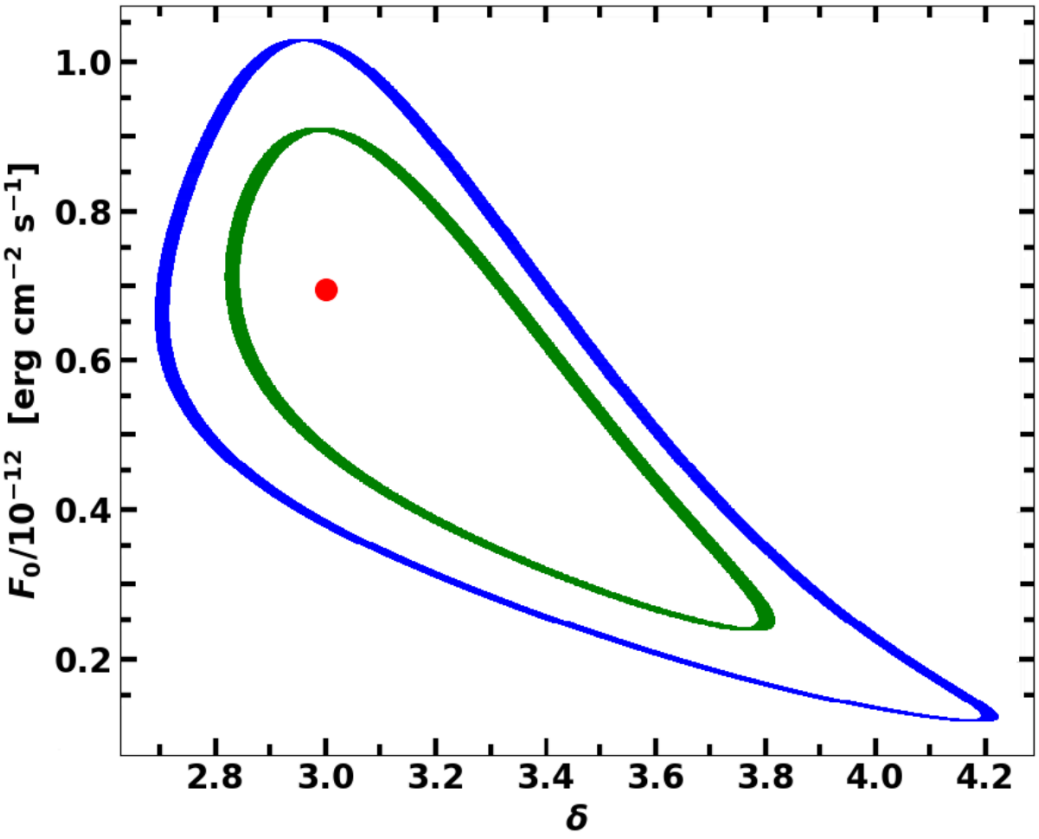

Figure 2.1: Countour green corresponds to the error ellipse at $\chi^2_{min}+1$ (coverage probability of 68.27% for individual estimation of F_0 and δ), and contour blue corresponds to error ellipse $\chi^2_{min}+2.3$ (coverage probability of 68.27% for joint estimation of F_0 and δ).

by the MAGIC telescopes for the EHBL PGC 2402248. We estimate the optimal value of the spectral index (δ) by varying the normalization constant, F_0, in order to find the best-fitting values for the gamma-ray spectrum. The best fit is achieved with an F_0 of 0.7×10^{-12} erg cm^{-2} s^{-1} and a δ of 3.0, resulting in a minimized chi-squared value (χ^2_{min}) of 1.52.

The error ellipse with blue contour, shown in Fig. 2.1, it is defined as the representation of the 68.27% confidence intervals for the joint estimation of the two parameters (F_0 and δ) used in the analysis. It is obtained by varying one parameter while keeping the other frozen at its optimum value. The statistical errors obtained are $F_0 = (0.7^{+0.33}_{-0.32}) \times 10^{-12}$ erg cm^{-2} s^{-1} and

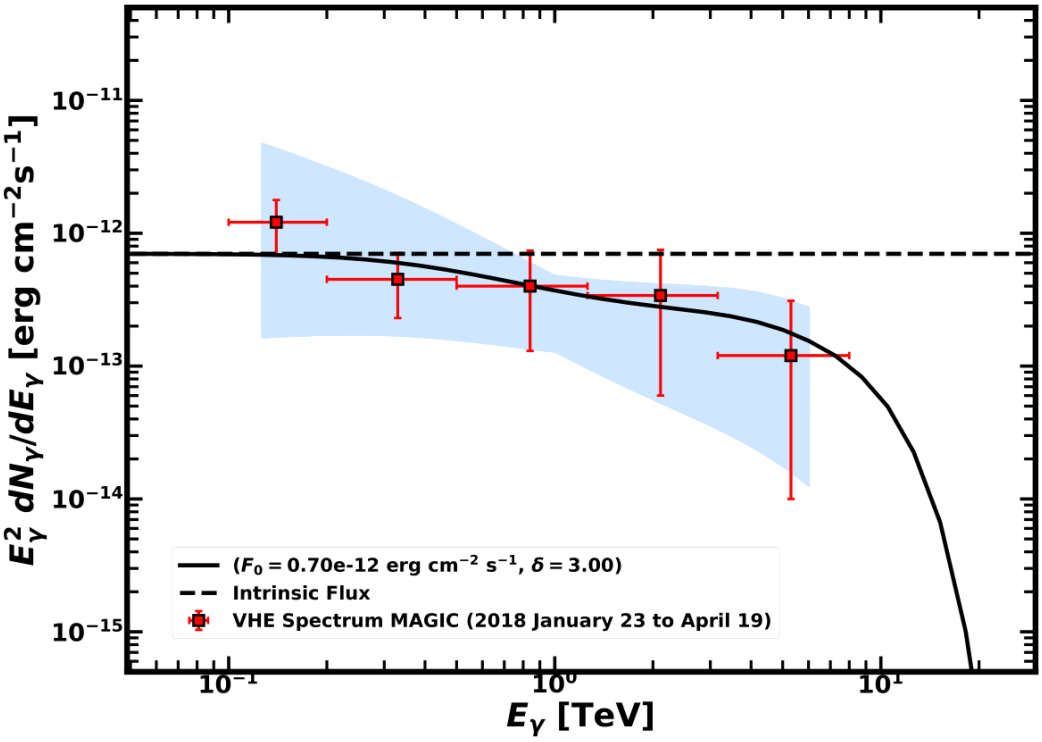

Figure 2.2: Fit to the VHE spectrum from the EHBL PGC 2402248, using the photohadronic model with the EBL model proposed by Franceschini et al. 2008. Shaded region corresponds to individual 1σ (68.27%) confidence level (CL) intervals of F_0 and δ, determined by the horizontal and the vertical tangents to the ellipse of $\chi^2_{min} + 1$, respectively. Dashed curve in this plot is the intrinsic flux.

$\delta = 3.0^{+0.40}_{-0.31}$. The Fig. 2.2 presents the best fit to the VHE spectrum of EHBL PGC 2402248 using the photohadronic model. The shaded region in the plot represents the 1σ (68.27%) confidence level region for the best-fit parameters (F_0 and δ), to determine this region we varied the values of F_0 and δ within their respective 68.27% confidence intervals. These confidence intervals were determined based by the ellipse $\chi^2_{min}+1$ (green contour) shown in Fig. 2.1. In addition, we have used different EBL models, specifically the ones proposed by Domínguez et al. 2011 and Gilmore et al. 2012, to fit the VHE spectrum and we have compared them with each other with the photohadronic model. Fig. 2.3 displays the results of these comparisons. All of these models fit the

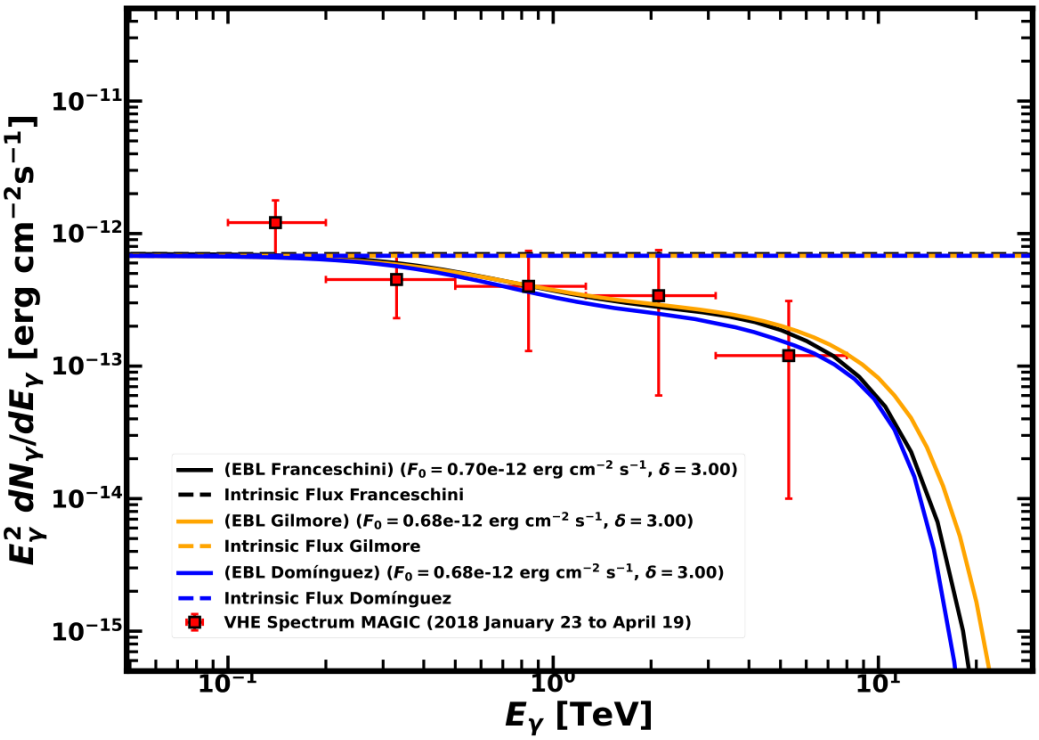

Figure 2.3: Photohadronic model fits comparison using Franceschini et al. 2008, Domínguez et al. 2011, and Gilmore et al. 2012, EBL's models. The dashed curves are the intrinsic fluxes.

observed data very well with $\delta = 3.0$ and nearly identical F_0 values. Small differences in fits above 1 TeV, as observed in our analysis. However, the different EBL models we have considered are compatible with each other. From now on, we used the EBL model of Franceschini et al. 2008 for comparison purposes, because the other EBL models yield similar results.

The observed VHE spectrum of the EHB PGC 2402248, which is significantly flat, suggests that its flux should increase substantially as the energy of gamma rays increases, particularly up to several TeV, and the spectrum should exhibit a hard spectral index (Costamante et al. 2018). However, the photohadronic model shown fitted to the VHE spectrum using a spectral index δ of 3.0, which corresponds to a state of low-emission and is characterized as soft (Sahu, Fortín, and Nagataki 2019). The intrinsic spectrum, represented by the dashed line in Figures 2.2 and 2.3, remains constant and

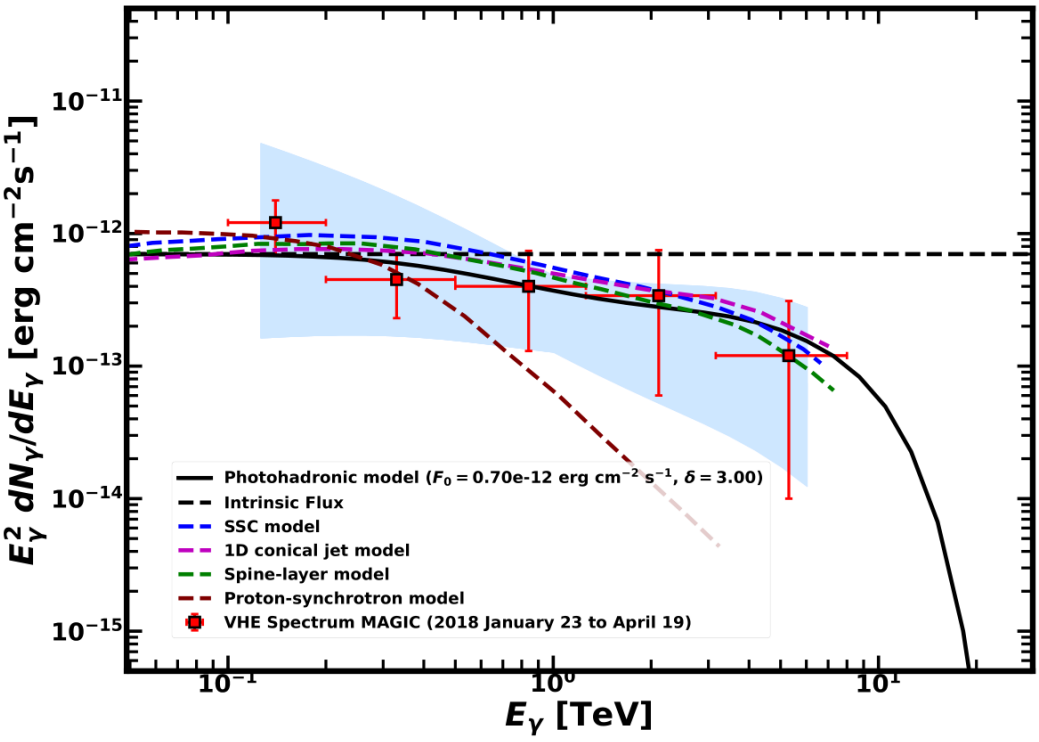

Figure 2.4: Comparison between leptonic, protron-synchrotron, and photohadronic models. Shaded region corresponds to individual 1σ-CL intervals of F_0 and δ. EBL model of Franceschini et al. 2008 was used.

is $F_\gamma = F_0$. The spectral index of the differential proton spectrum, α, is set to 2, which corresponds to a synchrotron spectral index $\beta = 1.0$. This implies that Φ_{SSC} is proportional to E_γ^{-1}.

In the work by Acciari et al. 2019, the SED of the blazar PGC 2402248 is analyzed using both leptonic and proton-synchrotron models. Specifically, the following leptonic models are considered: the 1D conical jet model, the spine-layer model and the one-zone SSC model. These models are used to fit the observed VHE spectrum of PGC 2402248 quite well, as illustrated in Fig. 2.4. Their behaviour is similar in the low- and high-energy limits. Nevertheless, in contrast to the leptonic models, the proton-synchrotron model does not provide a good fit to the observed spectrum and differs significantly from the fits obtained using the other models. In this model, the flux falls faster and earlier as energy increases. Among the various leptonic models

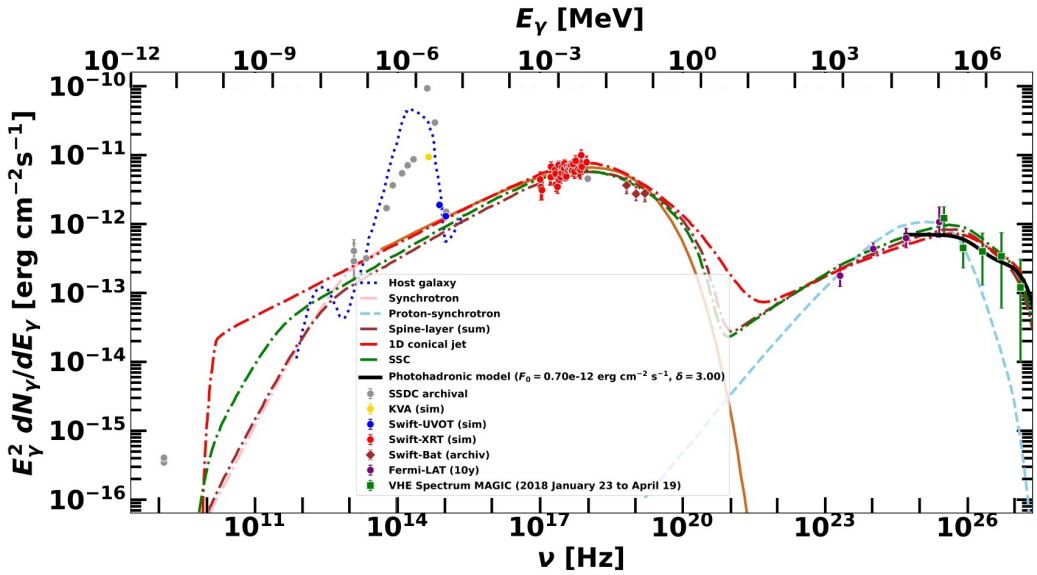

Figure 2.5: PGC 2402248 SED is fitted using the leptonic (One-zone SSC, 1D conical jet, and spine-layer) and the proton synchrotron models. The photohadronic model fit is shown for comparison.

used to fit the spectrum of PGC 2402248, it appears that the spine-layer model provides the best fit to the VHE region of the spectrum, with a χ^2_{min} value of 2.16. The photohadronic model provides a good fit to the observed spectrum, with a χ^2_{min} of 1.52. So, the comparison of the photohadronic model with different leptonic models (including the spine-layer model), indicates that the photohadronic fit is as good as or better than the leptonic model fits. Furthermore, the observation of a slight dip in the spectrum around the energy range of 1-2 TeV in the photohadronic models, which is less pronounced in the leptonic scenarios. Attributing the observed dip in the γ-ray spectrum to a slight dip in the EBL contribution around this region. We have shown the multiwavelength SED, in Fig. 2.5, with simultaneous data and archival data from different observations, alongside VHE fits from various models (the leptonic models, the proton-synchrotron model, and the photohadronic model). The Table 2.1 provided the important parameters used in all these models. According to Eq. 1.6, the energy range of γ-rays (E_γ) between 0.1 TeV and 8 TeV corresponds to Fermi accelerated proton energy (E_p) a range between 1 TeV and 80 TeV. To accelerate the protons

to energy $E_p \sim 80$ TeV within the inner jet region of radius $R'_f \sim 5 \times 10^{15}$ cm, the magnetic field B' can be estimated using the relation $eB' = E_p/R'_f$, which gives $B' \sim 0.5 \times 10^{-4}$ G. It is observed in Fig. 2.5 that the low-energy tail of the SSC band begins around of approximately $\epsilon_\gamma \simeq 10^{21}$ Hz. By using Eq. 1.7, we estimate the bulk Lorentz factor (remember that for HBLs $\Gamma \simeq \mathcal{D}$) based on the interaction of protons with energy $E_p \simeq 80$ TeV and SSC seed photons with energy $\epsilon_\gamma \simeq 4.1$ MeV to produce $E_\gamma \simeq 8$ TeV. We estimated the maximum value of $\Gamma \simeq 34$. As reported in the work of Acciari et al. 2019, the leptonic models take $\Gamma = 30$ to fit the broad band SED of PGC 2042248. Then, our estimate for the Γ is consistent with the value used in the leptonic model. The central black hole mass (MBH) is estimated to be approximately $(4.8 \pm 0.9) \times 10^8\ M_\odot$ (Becerra González, Acosta-Pulido, and Clavero 2020), as derived from velocity dispersion measurements. This measurement corresponds to an Eddington luminosity (L_{Edd}) in the range of approximately $(4.9 - 7.2) \times 10^{46}$ erg s^{-1}. The integrated VHE flux in the energy range of 0.13 TeV $\leq E_\gamma \leq$ 5.3 TeV is estimated to be approximately $F_\gamma \sim 4.3 \times 10^{-12}$ erg cm^{-2} s^{-1}, and furthermore, the VHE γ-ray luminosity (L_γ) associated with the source is estimated to be about $L_\gamma \sim 4.8 \times 10^{43}$ erg s^{-1}.

To estimate $\tau_{p\gamma}$ (the optical depth due to proton-photon interactions) and the photon density in the inner jet region, the following parameters are used (as reported in the study by Acciari et al. 2019): Inner jet radius (R'_f) is estimated to be approximately 5×10^{15} cm, and the outer jet radius (R'_b) is estimated to be around 10^{16} cm. A moderate efficiency of Δ-resonance production is assumed, and as a result, $\tau_{p\gamma}$ is expected to be less than 1, and with $\tau_{p\gamma} < 1$, it is estimated that the photon density in the inner jet region ($n'_{\gamma,f}$) is less than 4×10^{11} cm^{-3}. We can also constraint on the value of $\tau_{p\gamma}$ on the requirement that the Fermi-accelerated proton luminosity (L_p), which is responsible for producing VHE γ-rays, $L_p = 7.5\tau_{p\gamma}^{-1} L_\gamma$, should not exceed $L_{Edd}/2$. We take $L_{Edd} \sim 6.0 \times 10^{46}$ erg s^{-1}, and we obtain $\tau_{p\gamma} > 0.012$. For $\tau_{p\gamma} \sim 0.05$, the SSC photon density in the inner jet region is $n'_{\gamma,f} \sim 2.0 \times 10^{10}$ cm^{-3} and the proton luminosity is $L_p \sim 7.2 \times 10^{45}$ erg s^{-1}.

As previously discussed, in the photohadronic scenario, the relationship between the energy of neutrinos (E_ν) and the energy of γ-rays (E_γ) from the decay of charged pions is $E_\nu = 0.5E_\gamma$. For the VHE flare of PGC 2402248 on 2018 April 19, the maximum observed γ-ray energy (E_γ) was 8 TeV, and this corresponds to $E_\nu \sim 4$ TeV. This value of neutrino energy is relatively low, for neutrino detectors like IceCube to detect. We calculate the expected

neutrino flux from the observed VHE gamma-ray flux using Eq. 1.12. If the VHE γ-ray flux is $F_\gamma \sim 4.3\times10^{-12}$ erg cm^{-2} s^{-1}, which gives $F_\nu \sim 1.6\times10^{-12}$ erg cm^{-2} s^{-1}, which is also low. Thus, detecting low-energy neutrinos with a low neutrino flux can be challenging for the IceCube neutrino observatory.

Chapter 3

Constraining the redshift of VER J0521+211

In the period between 2009 to 2014, the VERITAS and MAGIC collaborations reported the observation of VHE flaring events coming from the BL Lac object VER J0521+211. The redshift is unknown, has been challenging to determine, and several analyses have provided different limits for it. In the context of the photohadronic model and utilizing three different EBL models, we have analyzed seven distinct VHE spectra of VER J0521+211. This analysis aims to determine the limiting values on its redshift. We observed that the analysis of the photohadronic scenario, when combined with the EBL model of Domínguez et al., has yielded excellent fits to the reported observations of VER J0521+211. Furthermore, photohadronic model has provided the most restrictive limits on the redshift z of this source: $0.29 \leq z \leq 0.31$ at 2σ, and $0.28 \leq z \leq 0.33$ at 3σ, confidence level (CL) intervals.

3.1 Multiwavelength observations

VERITAS collaboration conducted an analysis of γ-ray hot spots using data collected by the Fermi-LAT during its first year of operations (Errando 2011). These hot spots were not previously detected, at photon energies above 30 GeV. During the observation period from 2009 October 22 to 24 (MJD 55126–MJD 55128), a new VHE γ-ray source was discovered. This source was named VER J0521+211 and is associated with a radio and X-ray source known as RGB J0521.8+2112. VERITAS telescopes continued

its observations of VER J0521+211, accumulating data for a total exposure time of 14.5 h between 2009 October 22 and 2010 January 16. During this extended observation period, VERITAS detected a high-flux state on 2009 November 22 (MJD 55126–MJD 55212) (Archambault et al. 2013). VER J0521+211 is a highly variable source across all wavelengths, and it has an average integral flux $>$ 200 GeV. It is considered one of the brightest known blazars in the TeV energy range. Afterward, the categorization of VER J0521+211 as an IBL object is supported by the observation of a peak in its broad-band SED within the optical band. It is important to note that during the VHE γ-ray flare in 2009 November, it exhibited characteristics features that are typically associated with HBL objects (Ong 2009).

In the multiwavelength observations of VER J0521+211 conducted between 2012 November and 2014 February involved various observatories and instruments, including VERITAS, MAGIC, Fermi-LAT, Swift-XRT, and others. During this period, the source was found to be in a prolonged γ-ray flaring state (Adams et al. 2022). For a total of 23.6 h (after dead time corrections and data quality selection) VERITAS conducted observations to the source. Fermi-LAT observations of the source VER J0521+211 between 2012 October and 2014 May revealed variability in the γ-ray light curve at GeV energies. Between 2013 January 29 and 2014 January 24, Fermi-LAT observed a remarkable increase in the γ-ray flux from the source, approximately 11 times higher. Additionally, the monthly flux measurement was approximately 7 times larger than the values reported in the Fermi Large Area Telescope Third Source Catalogue (3FGL) published by Acero et al. 2015. This indicates that VER J052+521 was in a long-lasting elevated GeV γ-ray flux state. A moderate correlation was noted between the X-ray flux detected by the Swift-XRT (within the energy range of 0.3 to 10 keV) and the flux of TeV γ-rays.

During four nights, MAGIC telescopes carried out observations in the source: on October 15 and 16, as well as on November 29 and December 2, all in the year 2013. These observations acumulated a total effective time of 4.5 hours. During the evening of December 3, VERITAS conducted observations and detected a peak flux $>$200 GeV, with no intraday variability. However, specifically on December 2, MAGIC conducted observations and recorded a lower flux $>$200 GeV, as reported by Adams et al. 2022.

In the research conducted by Adams et al. 2022, they employed a Bayesian block analysis technique, which is a modeling method used to determine the optimal segmentation of the data within the observation interval (Scargle

et al. 2013). This technique was applied to analyze the VHE spectral curves observed by both VERITAS and MAGIC telescopes. Two change points, representing the boundaries of the Bayesian blocks, were identified on 2013 December 2 and 2013 December 6. These delineate three distinct Bayesian blocks as follows: BB1 (MJD 56580.0-MJD 56628.5; covering the period between 2013 December 2 and 2013 December 6), BB2 (MJD 56628.5-MJD 56632.5; covering the period between 2013 October 15 and 2013 December 2), and BB3 (MJD 56632.5-MJD 56689.0; covering the period between 2013 December 6 and 2014 February 1). Notably, the flux within each of these blocks remained constant, displaying no discernible flux variability. During the BB2 interval, there was only a single night of observation on December 3, 2013, conducted by VERITAS, lasting for approximately 2.3 h. The average flux recorded during this observation period was approximately 37% of the Crab Nebula flux, which stands as the highest among all the Bayesian blocks. Incorporating the results of the Bayesian block analysis conducted for the three distinct time intervals, and considering the construction of multiwavelength SEDs utilizing four different EBL models, Adams et al. 2022 established a conservative 95% confidence upper limit on the redshift, which is $z \leq 0.31$.

3.2 Results and analysis

VERITAS and MAGIC collaborations, between 2009 and 2014, conducted observations and notified primarily seven distinct periods of VHE γ-ray flaring from VER J0521+211. The fact that the redshift of VER J0521+211 is unknown has led to various analyses aimed at constraining its redshift. We apply the photohadronic model alongside three established EBL models to analyze these seven VHE spectra. The three parameters, of Eq. 1.11, the spectral index δ, the constant of normalization F_0, and the redshift z, are treated as variables and are simultaneously adjusted to find their optimal fit values. In Table 3.1 (from the third to the fifth column), the estimated parameters for the optimal fits are presented. Based on the optimal fit values of z, F_0, and δ, obtained using the three EBL models, we can determine the redshift CL intervals at 1σ, 2σ, and 3σ (shown in columns sixth, seventh, and eight of Table 3.1). As mentioned earlier, in our analysis, we constrain δ within the range $2.5 \leq \delta \leq 3.0$. For ease of reference, we have designated as V1 the VERITAS observations occurring from MJD 55126 (2009 octo-

Table 3.1: Estimated values for the parameters of the photohadronic model obtained from the best fits to the VHE spectra of VER J052+211. F_0 in units of $10^{-11}\,\mathrm{TeV\,cm^{-2}\,s^{-1}}$.

VER J0521+211	EBL	Parameters			Redshift CL intervals		
Observations	Model	F_0	δ	z	1σ	2σ	3σ
V1	Franceschini	2.05	2.52	0.29	(0.20, 0.32)	(0.18, 0.35)	(0.17, 0.36)
	Gilmore	1.80	2.62	0.30	(0.22, 0.35)	(0.19, 0.38)	(0.18, 0.39)
	Domínguez	2.05	2.51	0.28	(0.19, 0.31)	(0.17, 0.33)	(0.16, 0.34)
BB1	Franceschini	2.90	3.00	0.28	(0.27, 0.31)	(0.26, 0.34)	(0.25, 0.36)
	Gilmore	3.10	3.00	0.31	(0.29, 0.33)	(0.28, 0.37)	(0.27, 0.39)
	Domínguez	3.00	2.99	0.28	(0.26, 0.30)	(0.25, 0.33)	(0.24, 0.34)
BB2	Franceschini	5.30	3.00	0.25	(0.24, 0.29)	(0.23, 0.33)	(0.22, 0.35)
	Gilmore	5.45	3.00	0.27	(0.26, 0.31)	(0.25, 0.36)	(0.24, 0.38)
	Domínguez	5.20	3.00	0.24	(0.23, 0.27)	(0.22, 0.31)	(0.21, 0.33)
BB3	Franceschini	1.80	3.00	0.28	(0.25, 0.31)	(0.24, 0.35)	(0.23, 0.37)
	Gilmore	1.85	3.00	0.30	(0.27, 0.34)	(0.26, 0.38)	(0.25, 0.41)
	Domínguez	1.80	2.99	0.27	(0.25, 0.30)	(0.23, 0.33)	(0.22, 0.35)
MO15	Franceschini	8.50	2.79	0.37	(0.31, 0.44)	(0.29, 0.47)	(0.28, 0.47)
	Gilmore	11.1	2.70	0.42	(0.34, 0.48)	(0.31, 0.51)	(0.30, 0.52)
	Domínguez	9.10	2.77	0.37	(0.30, 0.43)	(0.28, 0.47)	(0.27, 0.48)
MO16	Franceschini	2.53	3.00	0.26	(0.21, 0.33)	(0.18, 0.40)	(0.17, 0.45)
	Gilmore	2.65	2.99	0.28	(0.23, 0.36)	(0.19, 0.44)	(0.18, 0.48)
	Domínguez	2.55	3.00	0.25	(0.21, 0.32)	(0.18, 0.39)	(0.17, 0.43)
MN29	Franceschini	6.55	2.93	0.34	(0.31, 0.39)	(0.30, 0.43)	(0.29, 0.44)
	Gilmore	5.90	2.99	0.35	(0.33, 0.42)	(0.29, 0.47)	(0.31, 0.48)
	Domínguez	5.75	2.98	0.32	(0.30, 0.37)	(0.29, 0.41)	(0.28, 0.43)

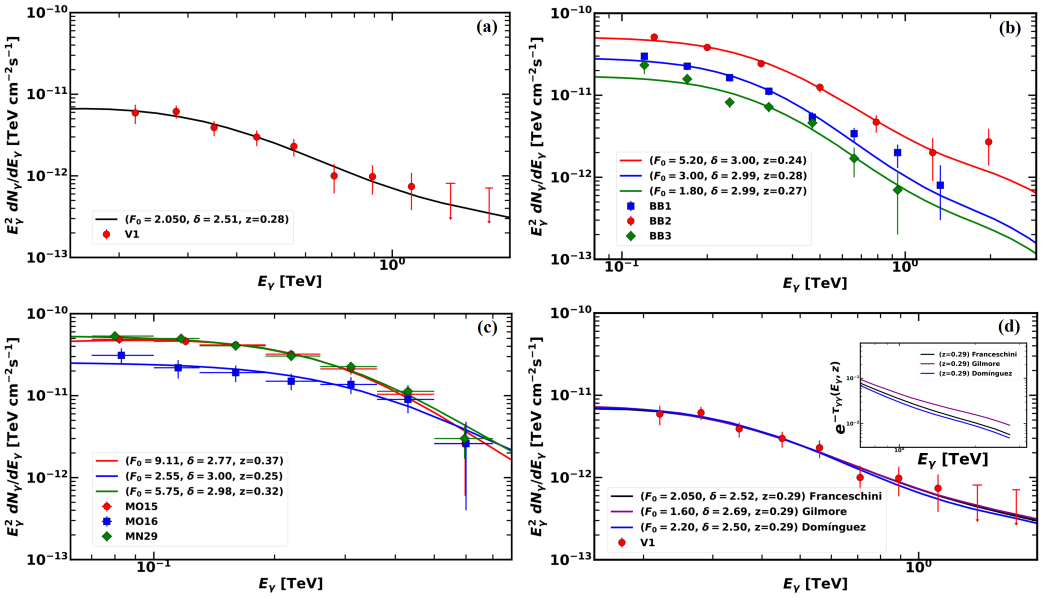

Figure 3.1: Fits to VHE γ-ray spectra of VER J0521+211 using the photohadronic model along with the EBL model proposed by Domínguez are given: (a) The time averaged spectrum V1. (b) The observed VHE γ-ray spectra BB1, BB2, and BB3. (c) The VHE γ-ray spectra MO15, MO16, and MN29. d) Using the three EBL models for comparison, the time averaged spectrum V1 is fitted for $z = 0.29$. In all cases, values of F_0 are in units of 10^{-11} TeV cm^{-2} s^{-1}.

ber 22) to MJD 55212 (2010 january 16), as documented by Archambault et al. 2013. Additionally, we labeled the VHE spectra recorded by MAGIC during three distinct nights: 2013 October 15 as MO15, 2013 october 16 as MO16, and 2013 November 29 as MN29. The three Bayesian blocks, namely BB1, BB2, and BB3, are described in Section 3.1. Once again, for the sake of convenience and simplicity, we define the EBL models used, as Franceschini (Franceschini et al. 2008), Domínguez (Domínguez et al. 2011), and Gilmore (Gilmore et al. 2012).

The time-averaged spectrum V1, as presented in Table 3.1, displays characteristics associated with a high emission state, $\delta = 2.5$, which are consistent with the fits provided by all EBL models. The EBL model proposed by Gilmore predicts a slightly elevated value for δ (2.62). Furthermore, it is noteworthy that each EBL model appears to yield slightly different predic-

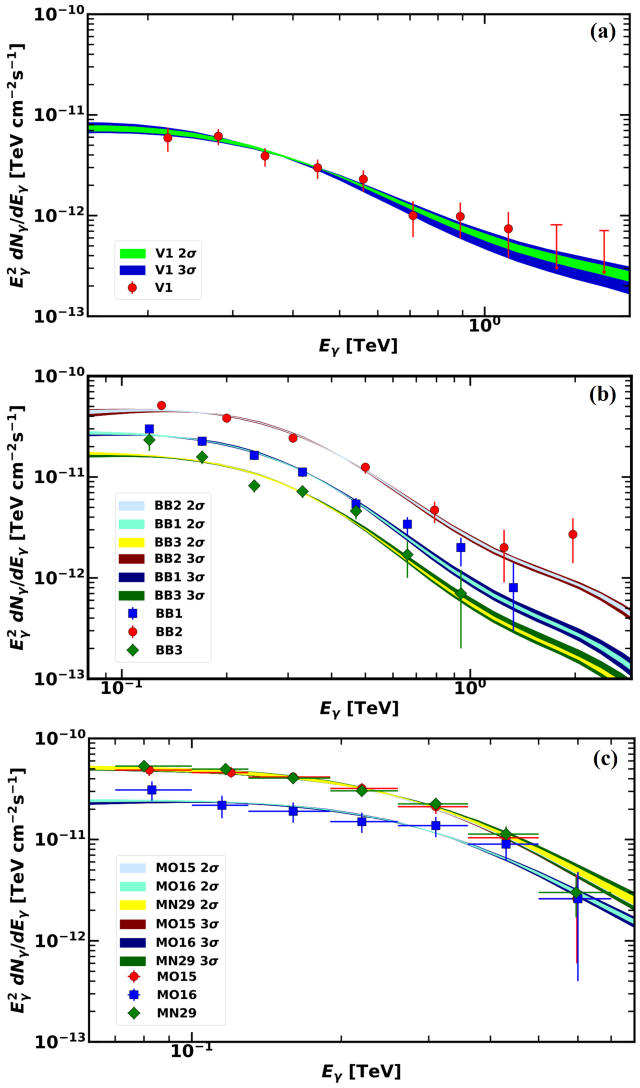

Figure 3.2: Fits to the seven observed VHE spectra of VER J0521+211 using the photohadronic model. The fits are performed separately at the limiting values of the CL overlapping regions of z for 2σ (0.29, 0.31) and 3σ (0.28, 0.33). The EBL model of Domínguez was used in this analysis. Fits are given as follows: a) V1 Spectrum, b) VHE γ-ray spectra of BB1, BB2, and BB3, and c) VHE γ-ray spectra of MO15, MO16, and MN29.

tions for the z associated with the flaring events. We employ the optimal

Table 3.2: Redshift overlapping CL regions of all the seven observations shown in Table 3.1.

EBL	1σ	2σ	3σ
Franceschini	-	(0.30, 0.33)	(0.29, 0.35)
Gilmore	-	(0.32, 0.36)	(0.31, 0.38)
Domínguez	-	(0.29, 0.31)	(0.28, 0.33)

parameters provided in Table 3.1 for Domínguez EBL model to perform fittings on the observed spectra, as depicted in Figs. 3.1 (a), (b), and (c). In Fig. 3.1(a) the fitting of the VHE spectrum V1, with the following parameter values: $z = 0.28, F_0 = 2.05 \times 10^{-11}$ TeV cm^{-2} s^{-1}, and $\delta = 2.51$. This δ value correspond to a state of very high emission. It is worth noting that during a roughly three-month period from 2009 October 22 to 2010 January 16, there was a sustained period of very high emission flaring. During this specific timeframe, there is a favourable opportunity to conduct a search for high-energy neutrinos originating from the direction of VER J0521+11 within the offline data of the IceCube 59 string configuration (IC59), as detailed in Aartsen, Abbasi, Abdou, et al. 2013, and Aartsen, Abbasi, Ackermann, et al. 2014. In Fig. 3.1(b) fittings for the VHE spectra BB1, BB2, and BB3, resulting in the following values of δ and z: (2.99, 0.28), (3.0, 0.24), and (2.99, 0.27), respectively. These δ values indicate that the spectra primarily correspond to low emission states. Also, in Fig. 3.1(c) VHE spectra MO15, MO16, and MN29 have been fitted using the respective optimal fit parameters as specified in Table 3.1.

To facilitate a meaningful comparison between the predictions of the three EBL models utilized, we have maintained a fixed redshift value of $z = 0.29$, and conducted fits to the VHE spectrum V1 using the photohadronic model, the results of these fits are represented in Figure 3.1(d). All the EBL models used exhibit excellent fits to the data. Nonetheless, by zooming in, particularly, for $E_\gamma \gtrsim 0.7$ TeV (as illustrated in the inset of Fig. 3.1(d)), where we have presented the VHE photon survival factor $e^{-\tau_{\gamma\gamma}}$ for each of the three models, it is noting that the EBL model proposed by Gilmore yields a slightly higher value. To conduct a comprehensive and complete analysis, we also determined the best-fits to the VHE spectra of the seven different flaring epochs observed by VERITAS and MAGIC, as listed in Table 3.1. These fits were carried out using the EBL models of Franceschini and Gilmore, and are presented in n Figs. A.1 to A.6 of Appendix A .

We take a specific EBL model and superimpose the 2σ CL intervals of z for all the seven observations listed in Table 3.1. This process is then repeated separately for the 1σ and 3σ CL intervals for each of the EBL models. The overlapping region in this analysis provides the limiting values of the z corresponding to a specific σ CL interval and the selected EBL model. We do not find these limits for the z within the 1σ CL intervals. Based on the overlapping regions of the redshift CL intervals presented in Table 3.2, it is evident that the EBL model proposed by Domínguez imposes the most stringent constraint on the z among the three EBL models considered. From the 2σ CL redshift overlapping region, the constraint on z is $0.29 \leq z \leq 0.31$, and from the 3σ CL overlapping region, the constraint is $0.28 \leq z \leq 0.33$. To date, no other analysis provides a stringent lower z limit for IBL VER J0521+211.

In the photohadronic model, we have utilized the redshift constraints derived from the EBL model of Domínguez, as indicated in Table 3.2, to fit the observed spectra. These fits are presented in figure 3.2 as follows: Fig. 3.2(a) contains the V1 spectrum, Fig. 3.2(b) includes the spectra BB1, BB2, and BB3, and Fig. 3.2(c) showcases the spectra MO15, MO16, and MN29. All the plots clearly illustrate the high quality of the photohadronic fits when taking into account the 2σ and/or 3σ overlapping regions as limiting for z.

Our research findings indicate that the flaring periods observed in IBL VER J0521+211 can be successfully fitted within the δ range of 2.5 to 3.0. It is important to note that the classification scheme and δ range were originally developed from the analysis of VHE spectra of HBLs (Sahu, Fortín, and Nagataki 2019). Additionally, it is noteworthy that our analysis relies on fitting the VHE spectra from seven independent observations.

Chapter 4

Deciphering the $\sim$ 18 TeV photons from GRB 221009A

GRB 221009A, an extremely powerful gamma-ray burst, was observed by multiple instruments on 2022 October 9. Despite the challenges posed by the interference from our Milky Way galaxy, the afterglow of GRB 221009A was exceptionally bright, surpassing the brightness of all previously observed GRBs. LHAASO (Large High Altitude Air Shower Observatory) detected several thousand VHE photons emitted by GRB 221009A, these high-energy photons extended up to 18 TeV. Detection of such high-energy photons is unexpected because of the significant opacity of the universe to VHE γ-rays. It is plausible that during the afterglow phase of GRB 221009A, the intrinsic VHE photon flux from the source experienced a substantial increase. This boost in intrinsic brightness might have compensated the attenuation by pair production with the EBL. We propose a scenario where VHE photons can be observed on Earth as a result of the interaction between VHE protons and seed synchrotron photons in the external forward shock region of a GRB jet.

4.1 Observations

At T_0= 13:16:59.000 UT on 2022 October 9 (Veres et al. 2022), a long-duration GRB designated as GRB 221009A (or Swift J1913.1+1946) in the direction of the Sagitta constellation was observed. This observation was made using the Gamma-ray Burst Monitor (GBM; Meegan et al. 2009) instrument aboard the Fermi Gamma-ray Space Telescope. The prompt emis-

sion of GRB 221009A was not only observed by the GBM but also by several other space observatories, such as: the Fermi-LAT, the AGILE (Piano et al. 2022; Ursi et al. 2022), the SRG (Lapshov et al. 2022), the GRBAlpha (Ripa et al. 2022), the Swift (Dichiara et al. 2022; Krimm et al. 2022), the INTEGRAL (Gotz et al. 2022), the Konus (Frederiks et al. 2022), the STPSat-6 (Mitchell, Philips, and Johnson 2022), and the Solar Orbiter (Xiao, Krucker, and Daniel 2022). GRB 221009A is positioned at the coordinates R.A. = 288.282 and decl. = 19.495, as reported in Pillera et al. 2022. At $T_0 + 240$ s the Fermi-LAT detected a photon with an energy of 99.3 GeV. this photon represents the highest-energy photon ever observed by Fermi-LAT during the prompt phase of a GRB (Bissaldi et al. 2022; Pillera et al. 2022). The afterglow emission of GRB 221009A was also observed at various wavelengths, as mentioned in the work of Das and Razzaque 2023, in addition, the optical follow-up observations indicated a very low redshift value of $z \simeq 0.151$, as reported in de Ugarte Postigo et al. 2022. In the works of de Ugarte Postigo et al. 2022, and Kann and Agui Fernandez 2022, reported that the estimated total emitted isotropic-equivalent gamma-ray energy from GRB 221009A is approximately in the range of $(2 - 6) \times 10^{54}$ erg. GRB 221009A is the brightest long-duration GRB and is considered one of the nearest, and possibly the most energetic one ever observed. Furthermore, it is noteworthy that GRB 221009A had a profound impact on Earth's lower ionosphere, specifically in the altitude range of approximately 60 to 100 kilometers (Hayes and Gallagher 2022), and it is reported to be the strongest ionization effect ever recorded from a GRB.

The detection of more than 5000 VHE photons by the LHAASO with its Water Cherenkov Detector Array (WCDA) and the larger Air Shower Kilometer Square Area (KM2A) detector within a time window of $T_0 + 2000$ s, these VHE photons were detected in the energy range spanning from 500 GeV to 18 TeV (Huang et al. 2022). The detection reported by the ground-based Cherenkov detector Carpet-2, situated at the Baksan Neutrino Observatory, an air shower that unequivocally originated from a photon with an extraordinary energy of 251 TeV, this event occurred 4536 seconds after the initial trigger by the GBM from the direction of GRB 221009A (Dzhappuev et al. 2022). Observations of these VHE γ-rays by both LHAASO and Carpet-2 from GRB 221009A have indeed raised intriguing questions and prompted speculation about possible nonstandard physics explanations for these observed events. It is important to acknowledge the caveat associated with the observation of the 251 TeV γ-ray. The angular resolution of the Carpet-2 de-

tector is several degrees, and the fact that two previously reported Galactic VHE sources, 3HWC J1928+178 and LHASSO J1929+1745, are situated in close proximity to the position of GRB 221009A, as noted by Fraija, Gonzalez, et al. 2022. The origin of the observed 251 TeV photon is indeed shrouded in uncertainty and the question of whether it is associated with GRB 221009A or either of the nearby Galactic sources. However, the temporal and spatial coincidence of the observed 251 TeV photon with GRB 221009A presents an intriguing avenue for exploration and scientific inquiry (Alves Batista 2022; Finke and Razzaque 2023; Mirabal 2023).

4.2 Common features of Blazars and GRBs

Blazars (a subclass of AGNs) and GRBs have common features shared between the emission mechanisms (Urry and Paolo Padovani 1995; Gehrels and Razzaque 2013). These common features are found to prevail in the synchrotron luminosity and Doppler factor (Wu, Zou, et al. 2011). In several works, the jets in GRBs and Blazars exhibit common features, despite the differences in their bulk Lorentz factors and masses (J. Wang and Wei 2010; Nemmen et al. 2012; Wu, Zhang, et al. 2016). Then, it is natural to use the mechanisms and processes observed to study the multi-TeV flaring of HBLs to study the afterglow phases of GRBs.

Previous works used the photohadronic process to investigate the multi-TeV flaring in HBLs (Sahu 2019; Sahu, Fortín, and Nagataki 2019; Sahu and Fortín 2020). In the context of the photohadronic scenario, protons within the blazar jet undergo acceleration to reach VHEs. Following this acceleration, these high-energy protons collide with background seed photons. This collision process results in the production of a Δ-resonance, through $p + \gamma \rightarrow \Delta^+$, and this process follow the kinematic condition indicated in Eq. (1.7). The Δ-resonances produced in the collision process eventually decay into π^0. These neutral pions subsequently decay to $\pi^0 \rightarrow \gamma\gamma$, producing VHE γ-rays, and, once produced, are blueshifted and then observed by Cherenkov telescopes on Earth. This model has demonstrated considerable success in explaining the VHE γ-ray spectra observed from many HBLs. In the context of this model, the intrinsic flux (F_{in}) (from Eq. 1.11) can be rewritten as

$$F_{in}(E_\gamma) = F_0 \, E_{\gamma,\mathrm{TeV}}^{-\delta+3}, \tag{4.1}$$

here $E_{\gamma,\mathrm{TeV}}$ represents the photon energy, is given in units of TeV. F_0 is the

normalization constant that can be determined from the observed spectrum, and δ is the spectral index, which is a free parameter in the model (Sahu 2019; Sahu, Fortín, and Nagataki 2019). The parameter F_{in}, is noted to be independent of the bulk Lorentz factor (Γ) and the Doppler factor ($\mathcal{D}$) of the source. For HBLs, it is observed that the seed photon flux (Φ_γ) follows a power-law behavior expressed as $\Phi_\gamma \propto \epsilon_\gamma^\beta \propto E_\gamma^{-\beta}$ (Sahu 2019; Sahu, Fortín, and Nagataki 2019). For HBLs, the spectral index δ, always falls within the range $2.5 \leq \delta \leq 3.0$. This range corresponds to a β value in the range $0.5 \leq \beta \leq 1.0$. The value of δ being within this range indicates that the seed photons are in the low-energy tail region of the SSC spectrum (Sahu, Fortín, and Nagataki 2019). In the context of GRBs, recent studies, as indicated by Sahu and Fortín 2020, have shown that the value of the parameter β can be either positive or negative. When $\beta > 0$, it implies that the seed photons are in the SSC regime, and when $\beta < 0$, it indicates that the seed photons are in the synchrotron regime. In previous studies of Sahu and Fortín 2020, and Sahu, Polanco, and Rajpoot 2022, the analysis of the VHE spectra of GRB 190114C and GRB 190829A, indicated that the production of VHE γ-rays in these GRBs is attributed to the interaction of high-energy protons with the low-energy tail region of the background SSC photons with the parameter $\beta > 0$. Also, the study conducted by Sahu and Fortín 2020 on the VHE spectrum of GRB 180720B revealed that the production of VHE γ-rays is attributed to the interaction of high-energy protons with the synchrotron seed photons within the GRB jet with $\beta < 0$. This negative value of β indicates that the seed photons involved in the photohadronic interactions primarily originated from the falling part of the synchrotron spectrum.

4.3 Results and analysis

LHAASO, employing its two detectors, WCDA and KM2A, achieved the successful detection of over 5000 photons with energies exceeding 500 GeV from GRB 221009A approximately $T \sim 2000$ s from the prompt emission. The quantity of photons, denoted as N_γ, detected during a time interval T by any of these detectors with a zenith angle θ and within the effective area $A(E_\gamma, \theta)$ (documented in Zhao, Zhou, and S. Wang 2023), is

$$N_\gamma = T \int_{0.5\ TeV} \frac{dN_\gamma}{dE_\gamma} A(E_\gamma, \theta)\ e^{-\tau_{\gamma\gamma}(E_\gamma, z)} dE_\gamma \tag{4.2}$$

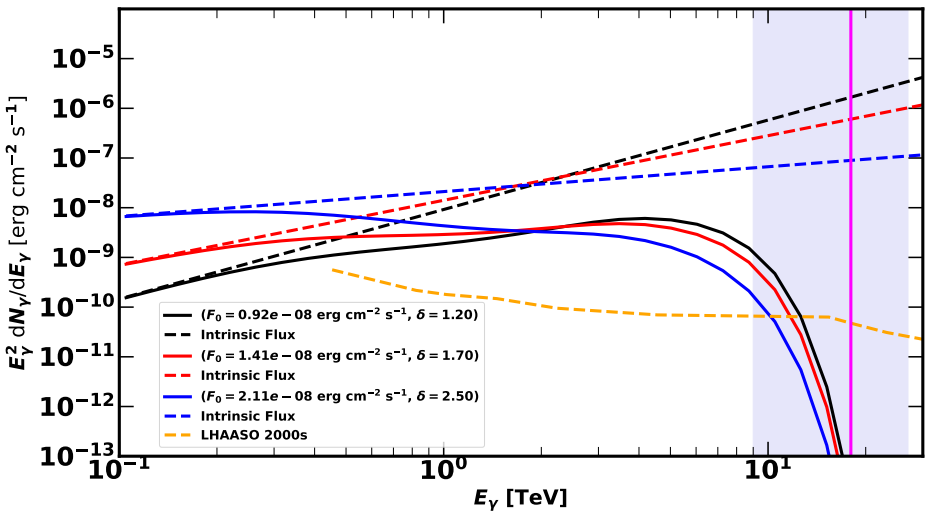

Figure 4.1: LHAASO-WCDA detector. $N_\gamma = 5500$, $\delta = 1.20, 1.70, 2.50$ (shaded region: $\pm 50\%$ relative energy resolution for $E_\gamma \simeq 18$ TeV).

Table 4.1: Behavior of VHE spectrum. For $\delta = 2.5, 1.70, 1.20$, and $N_\gamma = 5500, 6500$, the flux normalization factor F_0, the integrated flux F_γ^{int} in the energy range 100 GeV to 18 TeV (bothin 10^{-8} erg cm^{-2} s^{-1}), the corresponding luminosity $L_{\gamma,48}$ (in 10^{48} erg s^{-1}), and E_{cut} (in TeV; the value of E_γ where it intersects the LHAASO sensitivity curve with 2000 s exposure time), are presented using the LHAASO-WCDA and LHAASO-KM2A (bracketed values) effective detector areas ($30° \leq \theta \leq 45°$).

δ	N_γ	F_0	F_γ^{int}	$L_{\gamma,48}$	E_{cut}
2.5	5500	2.11 (0.54)	2.49 (0.63)	1.63 (0.41)	9.94 (8.17)
	6500	2.50 (0.63)	2.95 (0.75)	1.92 (0.49)	10.18 (8.41)
1.7	5500	1.41 (0.48)	1.22 (0.41)	0.80 (0.27)	11.53 (10.48)
	6500	1.67 (0.56)	1.44 (0.49)	0.94 (0.32)	11.70 (10.63)
1.2	5500	0.92 (0.36)	1.07 (0.42)	0.70 (0.27)	12.44 (11.32)
	6500	1.08 (0.42)	1.26 (0.50)	0.83 (0.32)	12.55 (11.50)

here, the differential photon spectrum can be expressed as follows

$$\frac{dN_\gamma}{dE_\gamma} = F_0\ E_{\gamma,\mathrm{TeV}}^{-\delta+1}\ \mathrm{TeV}^{-2} \tag{4.3}$$

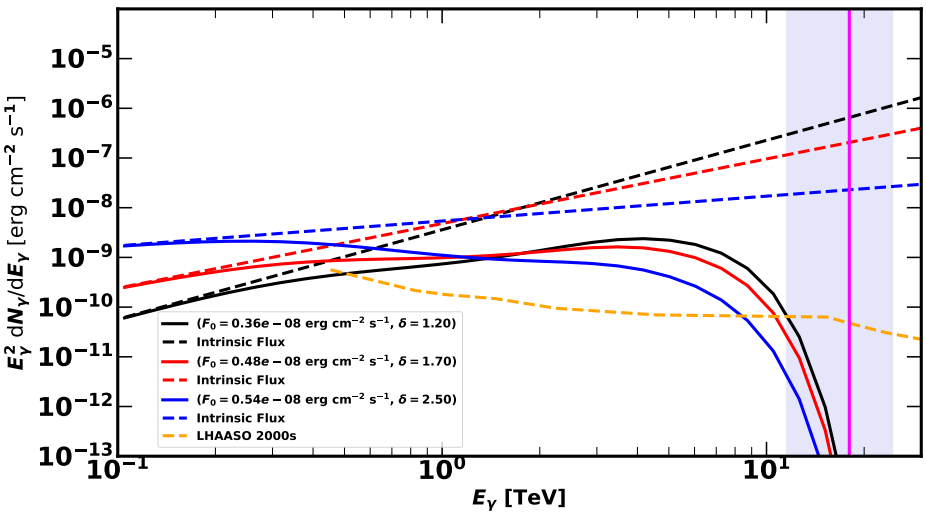

Figure 4.2: LHAASO-KM2A detector. $N_\gamma = 5500$, $\delta = 1.20, 1.70, 2.50$ (shaded region: $\pm 36\%$ relative energy resolution for $E_\gamma \simeq 18$ TeV).

The source was observed at a zenith angle within the range of 30° to 35°, and taking into account the effective areas of LHAASO-WCDA and LHAASO-KM2A (as outlined in Z. Cao et al. 2022), we calculate the integral in Eq. 4.2 for the values of δ equal to 1.2, 1.7, and 2.5. In the current analysis, we take into consideration the EBL model proposed by Franceschini et al. 2008. In our analysis, we assume that both detectors observe photons with energies above 500 GeV the range 5000 to 6500, denoted as N_γ. Once we fix the value of N_γ within this specified range, we proceed to calculate the corresponding value of F_0, this value is subsequently used to calculate the VHE photon flux and the integrated flux $F_\gamma^{\rm int}$ over the energy range of 100 GeV to 18 TeV. In Fig. 4.1, we present the predicted spectra for δ values: 1.2, 1.7, and 2.5. These predictions are made while considering the effective area of the LHAASO-WCDA detector and keeping N_γ fixed at a value of 5500. With a relative energy resolution of approximately 50% at energies around 18 TeV, as indicated in Figure 26 of Z. Cao et al. 2022. For δ value equal to 2.5, the photon flux begins at a peak value of F_γ around 10^{-8} erg cm^{-2} s^{-1} at $E_\gamma = 100$ GeV, and then gradually decreases up to approximately 4 TeV. Beyond approximately 4 TeV, the flux decreases more rapidly, and

this decline is attributed to the EBL effect. With 2000 s exposure the VHE spectrum intersects with the sensitivity curve of LHAASO, at $E_{cut} = 9.94$ TeV (located at the lower edge of the energy resolution, specifically at 9 TeV). The choice of $\delta = 2.5$ corresponds to $\beta = 0.5$, which implies that the intrinsic flux (F_{in}) is proportional to $F_{in} \propto E^{0.5}_{\gamma,\mathrm{TeV}}$. This scenario involves that seed photons are located in the lower tail region of the SSC spectrum within the GRB jet. The interaction of accelerated high-energy protons within the jet with the seed photons leads to the production of VHE γ-rays. This scenario exhibits strong similarities to the VHE flaring observed in HBLs.

We proceed with the calculation for $\delta = 1.7$, corresponding to $\beta = -0.3$. As previously discussed, the negative value of the seed photon spectral index β indicates that the photons are in the descending part of the synchrotron spectrum as they move towards higher ϵ_γ values. In this part we obtained that $\Phi_\gamma \propto \epsilon_\gamma^{-0.3}$. In this scenario, the interaction of the high-energy protons with the seed photons stemming from the synchrotron radiation regime of the external forward shock region, subsequently leads to the production of γ-rays. The spectrum initiates with a flux of approximately $F_\gamma \sim 10^{-9}$ erg cm^{-2} s^{-1} for $E_\gamma = 100$ GeV. It then exhibits a gradual increase up to approximately 4 TeV, after which it falls more rapidly due to the dominant influence of the exponentially decaying factor from the EBL. The obtained curve intersects with the sensitivity curve of LHAASO at an $E_{cut} = 11.53$ TeV. Notably, the intrinsic flux increases as $F_{in} \propto E^{1.3}_{\gamma,\mathrm{TeV}}$.

Finally, we examine a smaller value of $\delta = 1.2$ (as depicted in Fig. 4.1). This choice of δ results in $\beta = -0.8$, and in the context of photohadronic model, this corresponds to $\Phi_\gamma \propto \epsilon_\gamma^{-0.8}$, representing the descending part of the synchrotron spectrum as it extends toward higher ϵ_γ values, similar to the behavior observed for $\delta = 1.7$. But, the seed synchrotron spectrum in the external forward shock region falls more rapidly compared to the case with $\delta = 1.7$. The spectrum increases and attains its maximum flux at E_γ approximately to 4.5 TeV. Subsequently, it exhibits an exponential decrease for large values of E_γ, and eventually intersecting the LHAASO sensitivity curve at an energy cutoff of $E_{cut} = 12.44$ TeV. In this case, the intrinsic flux behaves according to $E^{1.8}_{\gamma,\mathrm{TeV}}$.

We replicate the calculation using the effective area of LHAASO-KM2A for $\delta = 1.2$, 1.7, and 2.5, keeping N_γ fixed at 5500. The results are presented in Fig. 4.2. It is important to note that for 18 TeV photons, the relative energy resolution of LHAASO-KM2A is approximately 36% (as indicated in Figure 2 of Chapter 1 of Z. Cao et al. 2022). This resolution

range positions the observed photon energy within the range of 11.52 to 24.48 TeV. For a given value of δ, the spectral patterns in both LHAASO-WCDA and LHAASO-KM2A are similar. However, it is worth noting that the E_{cut} for LHAASO-KM2A is lower than that of LHAASO-WCDA. Specifically, the E_{cut} for LHAASO-KM2A is less than 11.52 TeV, and this suggests that LHAASO-KM2A may not have the capability to detect photons with energies in this range.

By fixing N_γ at both 5500 and 6500, we have studied how the behavior of the VHE spectrum varies with different photon numbers. We have calculated various parameters, including luminosity L_γ, F_0, E_{cut} values, and the integrated flux F_γ^{int} using the effective areas of the LHAASO-WCDA and LHAASO-KM2A detectors. These are provided in Table 4.1. The bracketed values in Table 4.1 represent the results obtained using LHAASO-KM2A. We can observe that the increase in N_γ from 5500 to 6500 results in an increase in all the calculated quantities. Knowing both, the maximum energy E_γ and N_γ is essential for predicting the VHE γ-ray spectrum of a source, and it is equally important to have an understanding of the contribution from the EBL.

As the value of δ decreases from 2.5 to 1.2 for a given value of N_γ, the maximum E_{cut} tends to increase and approaches to 18 TeV. Furthermore, reaching Ecut values around 18 TeV in γ-ray spectra, which correspond to a very stiff synchrotron spectrum when decreasing the value of δ, can pose severe problems for various reasons. Moreover, for a given δ, increasing the N_γ tends to lead to an increase in the observed E_{cut} value. Based on our analysis, it appears that the LHAASO-WCDA detector is more likely to detect photons with energies around 18 TeV compared to the LHAASO-KM2A detector. The observed dependence of E_{cut} on the parameter δ indicates that when high-energy protons interact with the descending part of the synchrotron seed photon spectrum, it is more likely to result in the production of γ-ray photons with energies around 18 TeV compared to when these protons interact with the low-energy tail region of the seed SSC photons in the GRB jet.

Conclusions

HBLs are known to undergo episodes of VHE γ-ray flaring on various timescales, and the exact mechanisms behind these flares are not yet fully understood. Additionally, these VHE γ-rays are significantly attenuated as they travel through the EBL. In this work, we derive a simple relation between the observed VHE flux and the intrinsic flux from HBLs. This was achieved by assuming that during flaring events, high-energy protons undergoing Fermi acceleration interact with seed photons within the inner compact region of the jet. These interactions give rise to the generation of Δ-resonance, which subsequently undergoes decay, resulting in the emission of γ-rays and neutrinos originating from intermediate π^0 and π^+ particles, respectively. Even though the photohadronic scenario is effective for energies $E_\gamma \gtrsim 100$ GeV, it is important to consider that at lower energy regime ($E_\gamma \lesssim 100$ GeV), contributions from leptonic processes significantly impact the observed spectrum. Consequently, our model may not provide a satisfactory fit to the data in the low-energy regime. In certain cases, we have noted that explaining the averaging of long-term VHE observations using the photohadronic model can be challenging. This difficulty arises for two main reasons: Firstly, γ-rays stemming from leptonic processes contribute to the spectrum in the low-energy range, and secondly, the practice of averaging over numerous unobserved short flares, combined with periods of low emission, leads to data contamination.

Numerous models have proven effective at explaining the observed broadband SEDs. However, many of these models rely on a multitude of assumptions and involve a large number of free parameters. Some of these assumptions and parameters can be difficult to realize in the jet environment. In contrast, the photohadronic scenario relies on straightforward and relatively simple assumptions that are most likely to be realized within the jet during the period of VHE emissions. Another noteworthy aspect of our model is that

it operates under the assumption of a power-law behavior for the background seed photons, and this assumption alone is sufficient to successfully match the observed spectrum. This means that it does not require the availability of simultaneous multiwavelength observations.

Chapter 2 of this work, is focused on the analysis of the blazar PGC 2402248 within the framework of the photohadronic model, employing various EBL models. The detection of multi-TeV γ-rays from PGC 2402248 on 2018 April 19, using the MAGIC telescopes, supplied invaluable data for the analysis. Additionally, during this period, the source was simultaneously observed across a broad spectrum of frequency bands. The observed synchrotron peak frequency during the period from 2018 January to April, along with the analysis of 10 years of archival data from Swift-XRT, conclusively demonstrates that PGC 2402248 consistently exhibits characteristics of an EHBL. The VHE spectrum observed from the source appears to have a flatter shape when compared to the spectra of several other EHBLs. The broad-band SED of PGC 2402248 was analyzed using several leptonic models as well as the proton-synchrotron model. It has been observed that the leptonic models have been successful in providing a good fit to the observed VHE spectra. Within the framework of the photohadronic model, it was shown that the flat VHE spectrum can be accurately fitted with a spectral index of $\delta = 3.0$. This spectral index corresponds to a low-emission state. Furthermore, the photohadronic fit was compared to other leptonic and hadronic fits, and it was concluded that the photohadronic model provided an equally good or better fit to the data. Then, the photohadronic model emerged as a successful explanatory framework for the enigmatic VHE spectra observed in numerous HBLs and EHBLs.

In chapter 3, the analysis of the VHE spectra of the source VER J0521+211 was conducted using the photohadronic model in conjunction with three well-established EBL models. The primary objective was to achieve a detailed understanding of the emission from the source and establish rigorous constraints on its redshift. Over the period between 2009 to 2014, the VERITAS and MAGIC collaborations carried out observations during seven distinct VHE γ-ray flaring episodes associated with the IBL VER J0521+211. Despite these observations, the redshift, z, of this source remains unconfirmed. However, multiple analyses were conducted, utilizing multiwavelength observations, to constrain the redshift. In this part of the work, the uncertainties related to determining the redshift of the source were estimated. These uncertainties depend on the values of the photohadronic model parameters, F_0 and δ. This

analysis was conducted individually for each one of the seven independent VHE observations of VER J0521+511, and for each of the considered EBL models. The CL intervals for z at different sigmas were considered the determining factors in identifying which EBL model places the most stringent limits on z. According to our analysis, it is shown that the photohadronic model with the EBL model proposed by Domínguez, results in z overlapping CL regions, the z overlapping 2σ CL region is $0.29 \leq z \leq 0.31$. The z overlapping CL region is $0.28 \leq z \leq 0.33$. The lower limits of 0.29 from the 2σ CL intervals and 0.28 from the 3σ CL intervals represent the most stringent lower limits for z that have been obtained so far for the IBL VER J0521+211. The results are based on the fitting to the VHE spectra from the seven independent observations of VER J0521+211.

Finally, in Chapter 4, the recent observation of $\sim$ 18 TeV photons by LHAASO from GRB 221009A has raised doubts about the applicability of well-known EBL models for explaining photons with energies exceeding 10 TeV at a redshift of $z \geq 0.151$, even though we have successfully applied these EBL models to explain the VHE spectra of many other TeV sources. The incompatibility between this observation and the well-known EBL models has indeed prompted the exploration of new physics solutions. However, it is important to note that the proposed photohadronic model, can still offer valuable insights into the problem. In the context of this model, the high-energy protons interacting with the synchrotron photon background in the GRB jet can produce photons with energies close to 18 TeV. We anticipate that all the explanations analyzed here are pending the publication of additional results of GRB 221009A, which should confirm or rule them out. Also, the photohadronic model offers an option, within the framework of the standard model of particle physics, to explain the very high energy spectra of these objects without the need for physics beyond the standard model.

Appendix A

Fits of VER J0521+211 with other models

This appendix shows the plots of the best fits to the VHE spectra of VER J0521+211 using the photohadronic model and the EBL models proposed by Franceschini et al. 2008 and Gilmore et al. 2012. The normalization constant, F_0, is given in units of 10^{-11} TeV cm^{-2} s^{-1}.

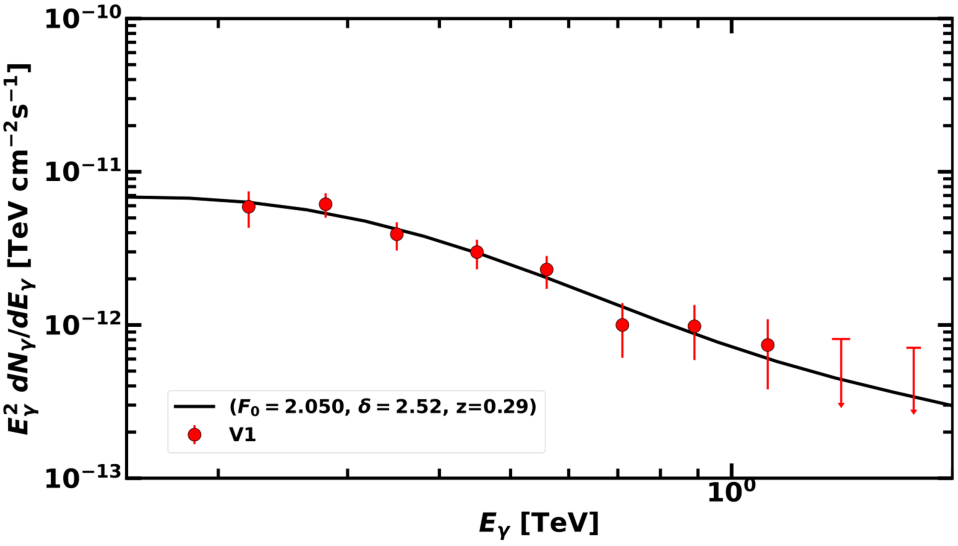

Figure A.1: Fit to the time-averaged VHE spectrum, V1, using the photo-hadronic model and the EBL model proposed by Franceschini.

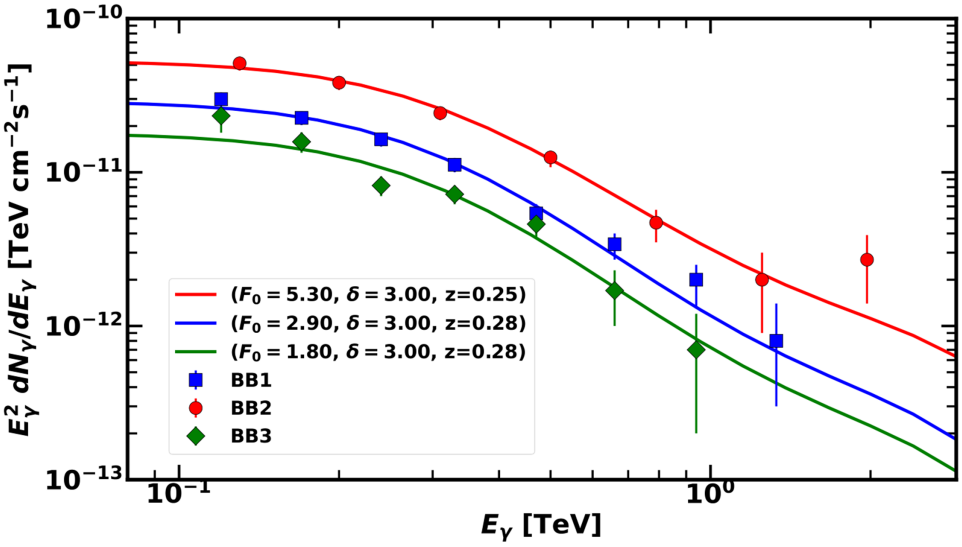

Figure A.2: Fit to the VHE spectra BB1, BB2, and BB3 with the photo-hadronic model along with the EBL model proposed by Franceschini.

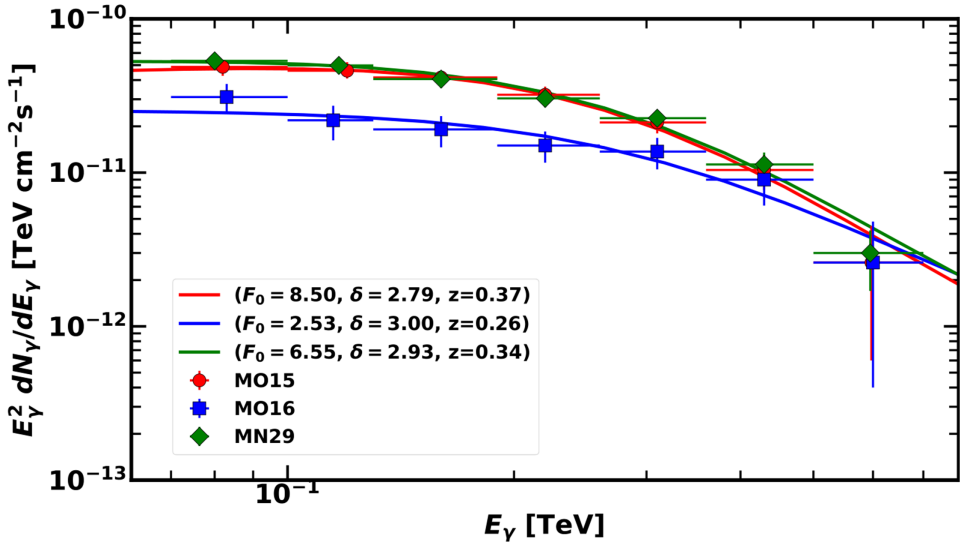

Figure A.3: Fit to VHE spectra MO15, MO16, and MN29, with the photohadronic model incorporating the EBL model proposed by Franceschini.

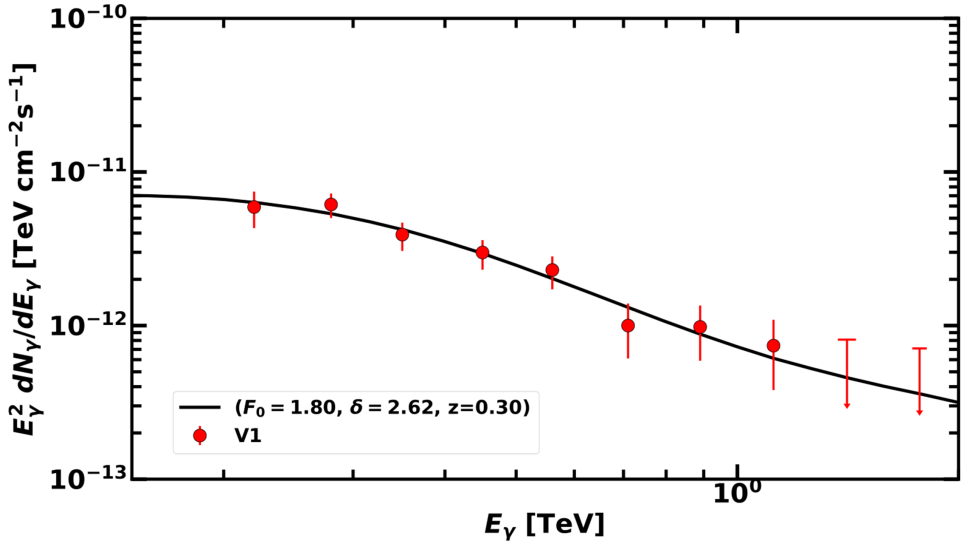

Figure A.4: Fit to the VHE spectrum, V1, using the photohadronic model incorporating the EBL model of Gilmore.

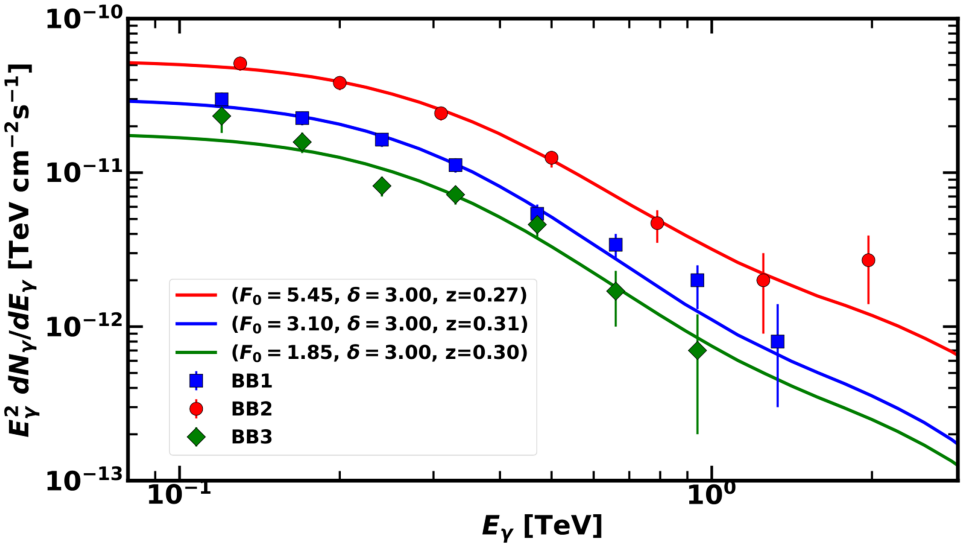

Figure A.5: Fit to VHE spectra BB1, BB2, and BB3 using the photohadronic model incorporating the EBL model of Gilmore.

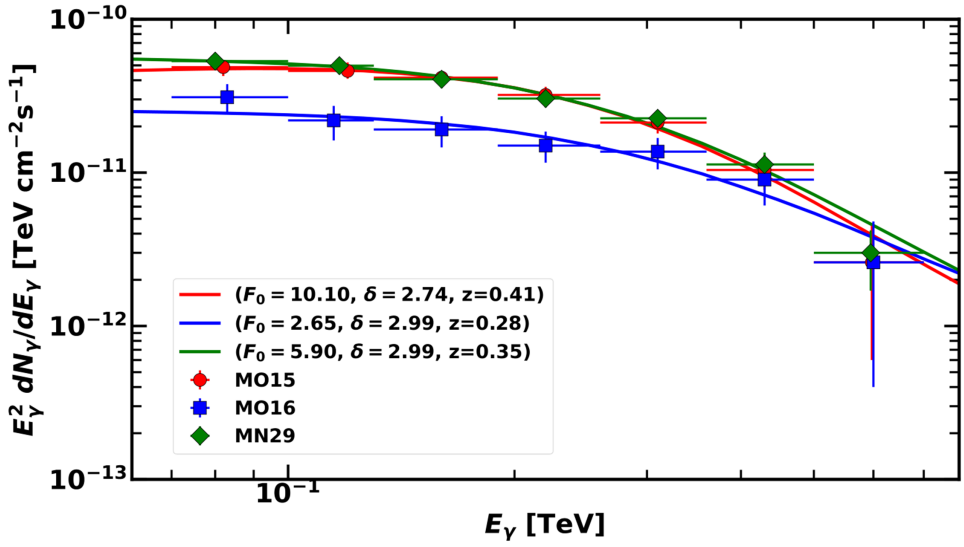

Figure A.6: VHE spectra MO15, MO16 and MN29 are fitted by including the EBL model of Gilmore to the photohadronic model.

Bibliography

Aartsen, M. G., R. Abbasi, Y. Abdou, et al. (Dec. 2013). "Search for time-independent Neutrino emission from astrophysical sources with 3 yr of IceCube DATA". In: *ApJ.* 779.2, p. 132. DOI: 10.1088/0004-637X/779/2/132. URL: https://dx.doi.org/10.1088/0004-637X/779/2/132.

Aartsen, M. G., R. Abbasi, M. Ackermann, et al. (Mar. 2014). "Search for a diffuse flux of astrophysical muon neutrinos with the IceCube 59-string configuration". In: *Phys. Rev. D.* 89 (6), p. 062007. DOI: 10.1103/PhysRevD.89.062007. URL: https://link.aps.org/doi/10.1103/PhysRevD.89.062007.

Abdo, A. A., M. Ackermann, I. Agudo, et al. (June 2010). "The Spectral Energy Distribution of Fermi bright blazars". In: *ApJ.* 716.1, p. 30. DOI: 10.1088/0004-637X/716/1/30. URL: https://dx.doi.org/10.1088/0004-637X/716/1/30.

Abdo, A. A., M. Ackermann, M. Ajello, W. B. Atwood, M. Axelsson, et al. (July 2009). "Bright Active Galactic Nuclei source list from the first three months of the Fermi Large Area Telescope all-sky suvey". In: *ApJ.* 700.1, p. 597. DOI: 10.1088/0004-637X/700/1/597. URL: https://dx.doi.org/10.1088/0004-637X/700/1/597.

Abdo, A. A., M. Ackermann, M. Ajello, W. B. Atwood, L. Baldini, et al. (Aug. 2010). "Fermi Large Area Telescope View of the Core of the Radio Galaxy Centaurus A". In: *ApJ.* 719.2, pp. 1433–1444. DOI: 10.1088/0004-637X/719/2/1433. arXiv: 1006.5463 [astro-ph.HE].

Acciari et al. (Sept. 2019). "Testing emission models on the extreme blazar 2WHSP J073326.7+515354 detected at very high energies with the MAGIC telescopes". In: *MNRAS.* 490.2, pp. 2284–2299. ISSN: 0035-8711. DOI: 10.1093/mnras/stz2725. eprint: https://academic.oup.com/mnras/article-pdf/490/2/2284/30257402/stz2725.pdf. URL: https://doi.org/10.1093/mnras/stz2725.

Acciari, V. A. et al. (Feb. 2011). "Spectral energy distribution of Markarian 501: Quiescent state versus extreme outburst". In: *ApJ.* 729.1, p. 2. DOI: 10.1088/0004-637X/729/1/2. URL: https://dx.doi.org/10.1088/0004-637X/729/1/2.

Acero, F. et al. (June 2015). "Fermi Large area telescope third source catalog". In: *ApJS.* 218.2, p. 23. DOI: 10.1088/0067-0049/218/2/23. URL: https://dx.doi.org/10.1088/0067-0049/218/2/23.

Ackermann, M. et al. (Nov. 2012). "The Imprint of the Extragalactic Background Light in the Gamma-Ray Spectra of Blazars". In: *Science* 338.6111, pp. 1190–1192. DOI: 10.1126/science.1227160. eprint: https://www.science.org/doi/pdf/10.1126/science.1227160. URL: https://www.science.org/doi/abs/10.1126/science.1227160.

Adams, C. B. et al. (June 2022). "Multiwavelength Observations of the Blazar VER J0521+211 during an Elevated TeV Gamma-Ray State". In: *ApJ.* 932.2, p. 129. DOI: 10.3847/1538-4357/ac6dd9. URL: https://dx.doi.org/10.3847/1538-4357/ac6dd9.

Aharonian, F. et al. (July 2007). "An Exceptional Very High Energy Gamma-Ray Flare of PKS 2155-304". In: *ApJL.* 664, pp. L71–L78. DOI: 10.1086/520635. arXiv: 0706.0797 [astro-ph].

Aharonian, F., A. Akhperjanian, and M. Beilicke (Nov. 2003). "Detection of TeV gamma-rays from the bl lac 1es1959+650 in its low states and during a major outburst in 2002". In: *A&A.* 406, pp. L9–L14. DOI: 10.1051/0004-6361:20030838. arXiv: astro-ph/0305275.

Aharonian, F. A. (Nov. 2000). "TeV gamma-rays from BL Lac objects due to synchrotron radiation of extremely high-energy protons". In: *New Astron.* 5, pp. 377–395. DOI: 10.1016/S1384-1076(00)00039-7. arXiv: astro-ph/0003159.

Aharonian, F. A., A. N. Timokhin, and A. V. Plyasheshnikov (Mar. 2002). "On the origin of highest energy gamma-rays from Mkn 501". In: *A&A.* 384, p. 834. DOI: 10.1051/0004-6361:20020062. arXiv: astro-ph/0108419.

Ajello, M. et al. (Aug. 2018). "Investigating the Nature of Late-time High-energy GRB Emission through Joint Fermi/Swift Observations". In: *ApJ.* 863.2, 138, p. 138. DOI: 10.3847/1538-4357/aad000.

Alves Batista, Rafael (Oct. 2022). "GRB 221009A: a potential source of ultra-high-energy cosmic rays". In: arXiv: 2210.12855 [astro-ph.HE].

Ansoldi, S. et al. (Aug. 2018). "The Blazar TXS 0506+056 Associated with a High-energy Neutrino: Insights into Extragalactic Jets and Cosmic-Ray

Acceleration". In: *ApJL.* 863.1, L10, p. L10. DOI: 10.3847/2041-8213/aad083. arXiv: 1807.04300 [astro-ph.HE].

Archambault, S. et al. (Sept. 2013). "Discovery of a new Tev gamma-ray source: VER J0521+211". In: *ApJ.* 776.2, p. 69. DOI: 10.1088/0004-637X/776/2/69. URL: https://dx.doi.org/10.1088/0004-637X/776/2/69.

Asano, Katsuaki and Masaaki Hayashida (July 2015). "The most intensive gamma-ray flare of Quasar 3C 279 with the second-order Fermi acceleration". In: *ApJL.* 808.1, p. L18. DOI: 10.1088/2041-8205/808/1/L18. URL: https://dx.doi.org/10.1088/2041-8205/808/1/L18.

— (June 2018). "Blazar Spectra with Hard-sphere-like Acceleration of Electrons". In: *ApJ.* 861.1, p. 31. DOI: 10.3847/1538-4357/aac82a. URL: https://dx.doi.org/10.3847/1538-4357/aac82a.

Asano, Katsuaki, Susumu Inoue, and Peter Mészáros (July 2009). "Prompt High-Energy Emission from Proton-Dominated Gamma-Ray Bursts". In: *ApJ.* 699.2, pp. 953–957. DOI: 10.1088/0004-637X/699/2/953. arXiv: 0807.0951 [astro-ph].

Asano, Katsuaki and Peter Mészáros (Oct. 2012). "Delayed Onset of High-energy Emissions in Leptonic and Hadronic Models of Gamma-Ray Bursts". In: *ApJ.* 757.2, 115, p. 115. DOI: 10.1088/0004-637X/757/2/115. arXiv: 1206.0347 [astro-ph.HE].

Becerra Gonzalez, J. et al. (May 2018). "Redshift determination of the very high energy gamma-ray extreme blazar PGC 2402248". In: *The Astronomer's Telegram* 11621, p. 1.

Becerra González, J, J A Acosta-Pulido, and R Clavero (Apr. 2020). "Optical spectral characterization of the TeV extreme blazar 2WHSP J073326.7+515354". In: *MNRAS.* 494.4, pp. 6036–6042. ISSN: 0035-8711. DOI: 10.1093/mnras/staa1144. eprint: https://academic.oup.com/mnras/article-pdf/494/4/6036/33212423/staa1144.pdf. URL: https://doi.org/10.1093/mnras/staa1144.

Bissaldi, E. et al. (Oct. 2022). "GRB 221009A or Swift J1913.1+1946: Fermi-LAT detection". In: *GRB Coordinates Network* 32637, p. 1.

Błażejowski, M. et al. (Dec. 2000). "Comptonization of Infrared Radiation from Hot Dust by Relativistic Jets in Quasars". In: *ApJ.* 545.1, p. 107. DOI: 10.1086/317791. URL: https://dx.doi.org/10.1086/317791.

Błażejowski., M. et al. (Sept. 2005). "A Multi-wavelength view of the TeV blazar Markarian 421: Correlated variability, flaring, and spectral evolu-

tion". In: *ApJ.* 630, pp. 130–141. DOI: 10.1086/431925. arXiv: astro-ph/0505325.

Böttcher, M. et al. (Apr. 2013). "Leptonic and Hadronic modeling of Fermi-detected blazars". In: *ApJ.* 768.1, p. 54. DOI: 10.1088/0004-637X/768/1/54. URL: https://dx.doi.org/10.1088/0004-637X/768/1/54.

Cao, Gang and Jiancheng Wang (Feb. 2014). "The Hadronic origin of the hard gamma-ray spectrum from Blazar 1ES 1101-232". In: *ApJ.* 783.2, p. 108. DOI: 10.1088/0004-637X/783/2/108. URL: https://dx.doi.org/10.1088/0004-637X/783/2/108.

Cao, Z. et al. (May 2022). "The Large High Altitude Air Shower Observatory (LHAASO) Science Book (2021 Edition)". In: *ChPhC.* 46, pp. 035001–035007. arXiv: 1905.02773 [astro-ph.HE].

Cerruti, M. et al. (Feb. 2015). "A hadronic origin for ultra-high-frequency-peaked BL Lac objects". In: *MNRAS.* 448.1, pp. 910–927. ISSN: 0035-8711. DOI: 10.1093/mnras/stu2691. eprint: https://academic.oup.com/mnras/article-pdf/448/1/910/9379400/stu2691.pdf. URL: https://doi.org/10.1093/mnras/stu2691.

Cerruti, Matteo (Sept. 2020). "Leptonic and Hadronic Radiative Processes in Supermassive-Black-Hole Jets". In: *Galaxies* 8.4, p. 72. DOI: 10.3390/galaxies8040072. arXiv: 2012.13302 [astro-ph.HE].

Chang, Y. L. et al. (Feb. 2017). "2WHSP: A multi-frequency selected catalogue of high energy and very high energy γ-ray blazars and blazar candidates". In: *A&A.* 598, A17. DOI: 10.1051/0004-6361/201629487. arXiv: 1609.05808 [astro-ph.HE].

Chary, Ranga-Ram and Alexandra Pope (Mar. 2010). "New Observational Constraints and Modeling of the Infrared Background: Dust Obscured Star-Formation at z> 1 and Dust in the Outer Solar System". In: *arXiv e-prints*, arXiv:1003.1731, arXiv:1003.1731. DOI: 10.48550/arXiv.1003.1731. arXiv: 1003.1731 [astro-ph.CO].

Costamante, L et al. (May 2018). "The NuSTAR view on hard-TeV BL Lacs". In: *MNRAS.* 477.3, pp. 4257–4268. ISSN: 0035-8711. DOI: 10.1093/mnras/sty857. eprint: https://academic.oup.com/mnras/article-pdf/477/3/4257/24820529/sty857.pdf. URL: https://doi.org/10.1093/mnras/sty857.

Costamante, L. et al. (May 2001). "Extreme synchrotron bl lac objects". In: *A&A.* 371, p. 512. DOI: 10.1051/0004-6361:20010412. arXiv: astro-ph/0103343.

Das, Saikat and Soebur Razzaque (Feb. 2023). "Ultrahigh-energy cosmic-ray signature in GRB 221009A". In: *A&A.* 670, p. L12. DOI: 10.1051/0004-6361/202245377. arXiv: 2210.13349 [astro-ph.HE].

de Ugarte Postigo, A. et al. (Oct. 2022). "GRB 221009A: Redshift from X-shooter/VLT". In: *GRB Coordinates Network* 32648, p. 1.

Derishev, Evgeny and Tsvi Piran (Aug. 2019). "The Physical Conditions of the Afterglow Implied by MAGIC's Sub-TeV Observations of GRB 190114C". In: *ApJL.* 880.2, L27, p. L27. DOI: 10.3847/2041-8213/ab2d8a. arXiv: 1905.08285 [astro-ph.HE].

Dermer, Charles D. and Reinhard Schlickeiser (Oct. 1993). "Model for the High-Energy Emission from Blazars". In: *ApJ.* 416, p. 458. DOI: 10.1086/173251.

Dichiara, S. et al. (Oct. 2022). "Swift J1913.1+1946 a new bright hard X-ray and optical transient". In: *GRB Coordinates Network* 32632, p. 1.

Domínguez, A. et al. (Jan. 2011). "Extragalactic background light inferred from AEGIS galaxy-SED-type fractions". In: *MNRAS.* 410.4, pp. 2556–2578. ISSN: 0035-8711. DOI: 10.1111/j.1365-2966.2010.17631.x. eprint: https://academic.oup.com/mnras/article-pdf/410/4/2556/6295256/mnras0410-2556.pdf. URL: https://doi.org/10.1111/j.1365-2966.2010.17631.x.

Dzhappuev, D. D. et al. (Oct. 2022). "Swift J1913.1+1946/GRB 221009A: detection of a 250-TeV photon-like air shower by Carpet-2". In: *ATel* 15669, p. 1.

Errando, M. (Nov. 2011). "Discovery and identification of two gamma-ray blazars at low galactic latitude with VERITAS". In: *arXiv e-prints*, arXiv:1111.1209. DOI: 10.48550/arXiv.1111.1209. arXiv: 1111.1209 [astro-ph.HE].

Finke, Justin D. and Soebur Razzaque (Jan. 2023). "Possible Evidence for Lorentz Invariance Violation in Gamma-Ray Burst 221009A". In: *ApJL.* 942.1, p. L21. DOI: 10.3847/2041-8213/acade1. arXiv: 2210.11261 [astro-ph.HE].

Finke, Justin D., Soebur Razzaque, and Charles D. Dermer (Feb. 2010). "Modeling the Extragalactic Background Light from Stars and Dust". In: *ApJ.* 712, pp. 238–249. DOI: 10.1088/0004-637X/712/1/238. arXiv: 0905.1115 [astro-ph.HE].

Fossati, G. et al. (Sept. 1998). "A unifying view of the spectral energy distributions of blazars". In: *MNRAS.* 299.2, pp. 433–448. DOI: 10.1046/j.1365-8711.1998.01828.x. arXiv: astro-ph/9804103 [astro-ph].

Fraija, Nissim, Magda Gonzalez, et al. (Oct. 2022). "Swift J1913.1+1946/GRB 221009A: Galactic sources of > 100 TeV-photon in spatial coincidence with the 250-TeV photon-like air shower reported by Carpet-2". In: *ATel.* 15675, p. 1.

Fraija, Nissim and Antonio Marinelli (Oct. 2016). "Neutrino, Γ-ray, and Cosmic-ray Fluxes From the Core of the Closest Radio Galaxies". In: *ApJ.* 830.2, p. 81. DOI: 10.3847/0004-637X/830/2/81. arXiv: 1607.04633 [astro-ph.HE].

Franceschini et al. (June 2008). "The extragalactic optical-infrared background radiations, their time evolution and the cosmic photon-photon opacity". In: *A&A.* 487, p. 837. DOI: 10.1051/0004-6361:200809691. arXiv: 0805.1841 [astro-ph].

Frederiks, D. et al. (Oct. 2022). "Konus-Wind detection of GRB 221009A". In: *GRB Coordinates Network* 32668, p. 1.

Gao, He et al. (Sept. 2013). "Compton scattering of self-absorbed synchrotron emission". In: *MNRAS.* 435.3, pp. 2520–2531. ISSN: 0035-8711. DOI: 10.1093/mnras/stt1461. eprint: https://academic.oup.com/mnras/article-pdf/435/3/2520/3431485/stt1461.pdf. URL: https://doi.org/10.1093/mnras/stt1461.

Gehrels, Neil and Soebur Razzaque (Dec. 2013). "Gamma-ray bursts in the swift-Fermi era". In: *Front. Phys.* 8.6, pp. 661–678. DOI: 10.1007/s11467-013-0282-3. arXiv: 1301.0840 [astro-ph.HE].

Ghisellini, G., A. Celotti, et al. (Dec. 1998). "A Theoretical unifying scheme for gamma-ray bright blazars". In: *MNRAS.* 301, p. 451. DOI: 10.1046/j.1365-8711.1998.02032.x. arXiv: astro-ph/9807317.

Ghisellini, G., G. Ghirlanda, et al. (Apr. 2010). "GeV emission from gamma-ray bursts: a radiative fireball?" In: *MNRAS.* 403.2, pp. 926–937. DOI: 10.1111/j.1365-2966.2009.16171.x. arXiv: 0910.2459 [astro-ph.HE].

Ghisellini, G., F. Tavecchio, and M. Chiaberge (Mar. 2005). "Structured jets in TeV BL Lac objects and radiogalaxies. Implications for the observed properties". In: *A&A.* 432.2, pp. 401–410. DOI: 10.1051/0004-6361:20041404. arXiv: astro-ph/0406093 [astro-ph].

Giannios, Dimitrios, Dmitri A. Uzdensky, and Mitchell C. Begelman (Feb. 2010). "Fast TeV variability from misaligned minijets in the jet of M87". In: *MNRAS.* 402, p. 1649. DOI: 10.1111/j.1365-2966.2009.16045.x. arXiv: 0907.5005 [astro-ph.HE].

Gilmore et al. (May 2012). "Semi-analytic modelling of the extragalactic background light and consequences for extragalactic gamma-ray spectra".

In: *MNRAS.* 422.4, pp. 3189–3207. ISSN: 0035-8711. DOI: 10.1111/j.1365-2966.2012.20841.x. eprint: https://academic.oup.com/mnras/article-pdf/422/4/3189/18601416/mnras0422-3189.pdf. URL: https://doi.org/10.1111/j.1365-2966.2012.20841.x.

Gotz, D. et al. (Oct. 2022). "GRB221009A/Swift J1913.1+1946: Integral SPI/ACS observations". In: *GRB Coordinates Network* 32660, p. 1.

Gupta, Nayantara (June 2008). "Gamma Rays from Centaurus A". In: *JCAP.* 06, p. 022. DOI: 10.1088/1475-7516/2008/06/022. arXiv: 0804.3017 [astro-ph].

Halzen, Francis and Dan Hooper (July 2005). "High energy neutrinos from the TeV blazar 1ES 1959+650". In: *Astropart. Phys.* 23, pp. 537–542. DOI: 10.1016/j.astropartphys.2005.03.007. arXiv: astro-ph/0502449.

Hauser, Michael G. and Eli Dwek (Sept. 2001). "The cosmic infrared background: measurements and implications". In: *Annu. Rev. Astron. Astrophys.* 39, pp. 249–307. DOI: 10.1146/annurev.astro.39.1.249. arXiv: astro-ph/0105539.

Hayes, Laura A. and Peter T. Gallagher (Oct. 2022). "A Significant Sudden Ionospheric Disturbance Associated with Gamma-Ray Burst GRB 221009A". In: *RNAAS.* 6.10, p. 222. DOI: 10.3847/2515-5172/ac9d2f. URL: https://dx.doi.org/10.3847/2515-5172/ac9d2f.

Holder, J. et al. (Jan. 2003). "Detection of TeV gamma rays from the BL Lacertae object 1ES 1959+650 with the Whipple 10-meter telescope". In: *ApJL.* 583, pp. L9–L12. DOI: 10.1086/367816. arXiv: astro-ph/0212170.

Huang, Yong et al. (Oct. 2022). "LHAASO observed GRB 221009A with more than 5000 VHE photons up to around 18 TeV". In: *GRB Coordinates Network* 32677, p. 1.

IceCube Collaboration et al. (July 2018). "Neutrino emission from the direction of the blazar TXS 0506+056 prior to the IceCube-170922A alert". In: *Science* 361.6398, pp. 147–151. DOI: 10.1126/science.aat2890. arXiv: 1807.08794 [astro-ph.HE].

Kann, D. A. and J. F. Agui Fernandez (Oct. 2022). "GRB 221009A: Armchair Energetics". In: *GRB Coordinates Network* 32762, p. 1.

Keshet, Uri and Eli Waxman (Mar. 2005). "Energy Spectrum of Particles Accelerated in Relativistic Collisionless Shocks". In: *Phys. Rev. Lett.* 94.11, 111102, p. 111102. DOI: 10.1103/PhysRevLett.94.111102. arXiv: astro-ph/0408489 [astro-ph].

Krawczynski, H. et al. (Jan. 2004). "Multiwavelength observations of strong flares from the TeV - blazar 1ES 1959+650". In: *ApJ.* 601, pp. 151–164. DOI: 10.1086/380393. arXiv: astro-ph/0310158.

Krimm, H. A. et al. (Oct. 2022). "GRB 221009A (Swift J1913.1+1946): Swift-BAT refined analysis". In: *GRB Coordinates Network* 32688, p. 1.

Kumar, P. and R. Barniol Duran (Nov. 2009). "On the generation of high-energy photons detected by the Fermi Satellite from gamma-ray bursts". In: *MNRAS.* 400.1, pp. L75–L79. DOI: 10.1111/j.1745-3933.2009.00766.x. arXiv: 0905.2417 [astro-ph.HE].

Kumar, Pawan and Bing Zhang (Feb. 2015). "The physics of gamma-ray bursts & relativistic jets". In: *Phys. Rep.* 561, pp. 1–109. DOI: 10.1016/j.physrep.2014.09.008. arXiv: 1410.0679 [astro-ph.HE].

Lapshov, I. et al. (Oct. 2022). "GRB221009A/Swift J1913.1+1946: SRG/ART-XC observation". In: *GRB Coordinates Network* 32663, p. 1.

Madau, Piero and Lucia Pozzetti (Feb. 2000). "Deep galaxy counts, extragalactic background light, and the stellar baryon budget". In: *MNRAS.* 312, p. L9. DOI: 10.1046/j.1365-8711.2000.03268.x. arXiv: astro-ph/9907315.

Maraschi, L., G. Ghisellini, and A. Celotti (Oct. 1992). "A Jet Model for the Gamma-Ray–emitting Blazar 3C 279". In: *ApJL.* 397, p. L5. DOI: 10.1086/186531.

Meegan, Charles et al. (Aug. 2009). "The Fermi Gamma-Ray-Burst monitor". In: *ApJ.* 702.1, p. 791. DOI: 10.1088/0004-637X/702/1/791. URL: https://dx.doi.org/10.1088/0004-637X/702/1/791.

Mirabal, N. (Feb. 2023). "Secondary GeV-TeV emission from ultra-high-energy cosmic rays accelerated by GRB 221009A". In: *MNRAS.* 519.1, pp. L85–L86. DOI: 10.1093/mnrasl/slac157. arXiv: 2210.14243 [astro-ph.HE].

Mitchell, L. J., B. F. Philips, and W. N. Johnson (Oct. 2022). "GRB 221009A: Gamma-ray Detection by SIRI-2". In: *GRB Coordinates Network* 32746, p. 1.

Mücke, A. et al. (Aug. 1999). "Photohadronic Processes in Astrophysical Environments". In: *PASA.* 16.2, pp. 160–166. DOI: 10.1071/AS99160. arXiv: astro-ph/9808279 [astro-ph].

Muecke, A. et al. (Mar. 2003). "BL Lac Objects in the synchrotron proton blazar model". In: *Astropart. Phys.* 18, pp. 593–613. DOI: 10.1016/S0927-6505(02)00185-8. arXiv: astro-ph/0206164.

Murase, Kohta et al. (Mar. 2012). "Blazars as ultra-high-energy cosmic ray sources: implications for TeV gamma-ray observations". In: *ApJ.* 749.1, p. 63. DOI: 10.1088/0004-637X/749/1/63. URL: https://dx.doi.org/10.1088/0004-637X/749/1/63.

Nemmen, R. S. et al. (Dec. 2012). "A Universal Scaling for the Energetics of Relativistic Jets from Black Hole Systems". In: *Science.* 338.6113, pp. 1445–1448. DOI: 10.1126/science.1227416. eprint: https://www.science.org/doi/pdf/10.1126/science.1227416. URL: https://www.science.org/doi/abs/10.1126/science.1227416.

Ong, Rene A. (Oct. 2009). "VERITAS discovery of a new VHE Gamma-ray Source, VER J0521+211". In: *The Astronomer's Telegram* 2260, p. 1.

Owen, Ellis R et al. (Aug. 2018). "Interactions between ultra-high-energy particles and protogalactic environments". In: *MNRAS.* 481.1, pp. 666–687. ISSN: 0035-8711. DOI: 10.1093/mnras/sty2279. eprint: https://academic.oup.com/mnras/article-pdf/481/1/666/25697897/sty2279.pdf. URL: https://doi.org/10.1093/mnras/sty2279.

Padovani, P. et al. (Aug. 2017). "Active galactic nuclei: what's in a name?" In: *A&AR.* 25.1, p. 2. DOI: 10.1007/s00159-017-0102-9. arXiv: 1707.07134 [astro-ph.GA].

Padovani, Paolo and Paolo Giommi (May 1995). "The Connection between X-Ray– and Radio-selected BL Lacertae Objects". In: *ApJ.* 444, p. 567. DOI: 10.1086/175631. arXiv: astro-ph/9412073 [astro-ph].

Petropoulou, M., S. Coenders, and S. Dimitrakoudis (July 2016). "Time-dependent neutrino emission from Mrk 421 during flares and predictions for IceCube". In: *Astropart. Phys.* 80, pp. 115–130. DOI: 10.1016/j.astropartphys.2016.04.001. arXiv: 1603.06954 [astro-ph.HE].

Petropoulou, M., K. Nalewajko, et al. (May 2017). "A hadronic minute-scale GeV flare from quasar 3C 279?" In: *MNRAS.* 467.1, pp. L16–L20. DOI: 10.1093/mnrasl/slw252. arXiv: 1612.05699 [astro-ph.HE].

Petropoulou, Maria et al. (Dec. 2017). "The many faces of blazar emission in the context of hadronic models". In: *14th Marcel Grossmann Meeting on Recent Developments in Theoretical and Experimental General Relativity, Astrophysics, and Relativistic Field Theories.* Vol. 3, pp. 3061–3067. DOI: 10.1142/9789813226609_0387. arXiv: 1601.06010 [astro-ph.HE].

Piano, G. et al. (Oct. 2022). "GRB 221009A (Swift J1913.1+1946): AGILE/GRID detection". In: *GRB Coordinates Network* 32657, p. 1.

Pillera, R. et al. (Oct. 2022). "GRB 221009A: Fermi-LAT refined analysis". In: *GRB Coordinates Network* 32658, p. 1.

Piran, Tsvi (Oct. 2004). "The physics of gamma-ray bursts". In: *Rev. Mod. Phys.* 76.4, pp. 1143–1210. DOI: 10.1103/RevModPhys.76.1143. arXiv: astro-ph/0405503 [astro-ph].

Rachen, Jorg P. (Aug. 2000). "Hadronic blazar models and correlated x-ray / TeV flares". In: *AIP Conf. Proc.* 515.1. Ed. by B. L. Dingus, M. H. Salamon, and D. B. Kieda, p. 41. DOI: 10.1063/1.1291342. arXiv: astro-ph/0003282.

Razzaque, Soebur (Nov. 2010). "A Leptonic-Hadronic Model for the Afterglow of Gamma-ray Burst 090510". In: *ApJL.* 724.1, pp. L109–L112. DOI: 10.1088/2041-8205/724/1/L109. arXiv: 1004.3330 [astro-ph.HE].

Razzaque, Soebur, Charles D. Dermer, and Justin D. Finke (Aug. 2010). "Synchrotron Radiation from Ultra-High Energy Protons and the Fermi Observations of GRB 080916C". In: *Open Astron.* 3.1, pp. 150–155. DOI: 10.2174/1874381101003010150. arXiv: 0908.0513 [astro-ph.HE].

Reimer, Anita, R. J. Protheroe, and A. -C. Donea (Apr. 2004). "M87 as a misaligned synchrotron - proton blazar?" In: *New Astron. Rev.* 48. Ed. by T. Kajita et al., pp. 411–413. DOI: 10.1051/0004-6361:20034231. arXiv: astro-ph/0402258.

Reynoso, M. M., M. C. Medina, and G. E. Romero (July 2011). "A lepto-hadronic model for high-energy emission from FR I radiogalaxies". In: *A&A.* 531, A30. DOI: 10.1051/0004-6361/201014998. arXiv: 1005.3025 [astro-ph.HE].

Rieger, F. M. and F. A. Aharonian (Feb. 2008). "Variable VHE gamma-ray emission from non-blazar AGNs". In: *A&A.* 479, p. L5. DOI: 10.1051/0004-6361:20078706. arXiv: 0712.2902 [astro-ph].

Rieger, Frank M. (Nov. 2011). "Non-thermal Processes in Black-Hole-Jet Magnetospheres". In: *Int. J. Mod. Phys. D* 20, pp. 1547–1596. DOI: 10.1142/S0218271811019712. arXiv: 1107.2119 [astro-ph.CO].

Rieger, Frank M. and Amir Levinson (June 2010). "TeV emission and jet formation in M87". In: *PoS.* TEXAS2010. Ed. by Frank M. Rieger, Christopher van Eldik, and Werner Hofmann, p. 047. DOI: 10.22323/1.123.0047.

Ripa, J. et al. (Oct. 2022). "GRB 221009A: Detection by GRBAlpha". In: *GRB Coordinates Network* 32685, p. 1.

Roustazadeh, P. and M. Böttcher (Feb. 2011). "Very High Energy Gamma-ray-induced Pair Cascades in the Radiation Fields of Dust Tori of Active Galactic Nuclei: Application to Cen A". In: *ApJ.* 728.2, 134, p. 134. DOI: 10.1088/0004-637X/728/2/134. arXiv: 1012.3923 [astro-ph.HE].

Sahu, Sarira (July 2019). "Multi-TeV flaring in nearby High Energy Blazars: A photohadronic scenario". In: *Rev. Mex. Fis.* 65.4, pp. 307–320. DOI: 10.31349/RevMexFis.65.307. arXiv: 1907.01174 [astro-ph.HE].

Sahu, Sarira and Carlos E. López Fortín (June 2020). "Origin of Sub-TeV Afterglow Emission from Gamma-Ray Bursts GRB 190114C and GRB 180720B". In: *ApJL.* 895.2, p. L41. DOI: 10.3847/2041-8213/ab93da. URL: https://dx.doi.org/10.3847/2041-8213/ab93da.

Sahu, Sarira, Carlos E. López Fortín, and Shigehiro Nagataki (Oct. 2019). "Multi-TeV Flaring from High-energy Blazars: An Evidence of the Photohadronic Process". In: *ApJL.* 884.1, p. L17. DOI: 10.3847/2041-8213/ab43c7. URL: https://dx.doi.org/10.3847/2041-8213/ab43c7.

Sahu, Sarira, Alberto Rosales de León, and Luis Salvador Miranda (Nov. 2017). "Photohadronic scenario in interpreting the February–March 2014 flare of 1ES 1011+496". In: *Eur. Phys. J. C* 77.11, p. 741. DOI: 10.1140/epjc/s10052-017-5335-2. arXiv: 1610.01709 [astro-ph.HE].

Sahu, Sarira, Andres Felipe Osorio Oliveros, and Juan Carlos Sanabria (May 2013). "Hadronic-origin orphan TeV flare from 1ES 1959+650". In: *Phys. Rev. D* 87 (10), p. 103015. DOI: 10.1103/PhysRevD.87.103015. URL: https://link.aps.org/doi/10.1103/PhysRevD.87.103015.

Sahu, Sarira, Isabel Abigail Valadez Polanco, and Subhash Rajpoot (Apr. 2022). "Very High-energy Afterglow Emission of GRB 190829A: Evidence for Its Hadronic Origin?" In: *ApJ.* 929.1, p. 70. DOI: 10.3847/1538-4357/ac5cc6. arXiv: 2204.04822 [astro-ph.HE].

Sari, Re'em and Ann A. Esin (Feb. 2001). "On the Synchrotron Self-Compton Emission from Relativistic Shocks and Its Implications for Gamma-Ray Burst Afterglows". In: *ApJ.* 548.2, pp. 787–799. DOI: 10.1086/319003. arXiv: astro-ph/0005253 [astro-ph].

Scargle, Jeffrey D. et al. (Feb. 2013). "Studies in astronomical time series analysis. VI. Bayesian block representations". In: *ApJ.* 764.2, p. 167. DOI: 10.1088/0004-637X/764/2/167. URL: https://dx.doi.org/10.1088/0004-637X/764/2/167.

Sikora, Marek, Mitchell C. Begelman, and Martin J. Rees (Jan. 1994). "Comptonization of Diffuse Ambient Radiation by a Relativistic Jet: The Source of Gamma Rays from Blazars?" In: *ApJ.* 421, p. 153. DOI: 10.1086/173633.

Stecker, F. W., O. C. de Jager, and M. H. Salamon (May 1992). "TeV gamma rays from 3C 279 - A possible probe of origin and intergalactic infrared radiation fields". In: *ApJL.* 390, p. L49. DOI: 10.1086/186369.

Summerlin, Errol J. and Matthew G. Baring (Jan. 2012). "Diffusive Acceleration of Particles at Oblique, Relativistic, Magnetohydrodynamic Shocks". In: *ApJ.* 745.1, 63, p. 63. DOI: 10.1088/0004-637X/745/1/63. arXiv: 1110.5968 [astro-ph.HE].

Tavecchio, Fabrizio, Laura Maraschi, and Gabriele Ghisellini (June 1998). "Constraints on the Physical Parameters of TeV Blazars". In: *ApJ.* 2, p. 608. DOI: 10.1086/306526. URL: https://dx.doi.org/10.1086/306526.

Urry, C. Megan and Paolo Padovani (Sept. 1995). "Unified schemes for radio-loud Active Galactic Nuclei". In: *PASP.* 107.715, p. 803. DOI: 10.1086/133630. URL: https://dx.doi.org/10.1086/133630.

Ursi, A. et al. (Oct. 2022). "GRB 221009A (Swift J1913.1+1946): AGILE/MCAL detection". In: *GRB Coordinates Network* 32650, p. 1.

Veres, P. et al. (Oct. 2022). "GRB 221009A: Fermi GBM detection of an extraordinarily bright GRB". In: *GRB Coordinates Network* 32636, p. 1.

Wang, J. and J. Y. Wei (Dec. 2010). "Gamma-Ray Burst afterglows as analogs of high-frequency-peaked BL Lac objects". In: *ApJL.* 726.1, p. L4. DOI: 10.1088/2041-8205/726/1/L4. URL: https://dx.doi.org/10.1088/2041-8205/726/1/L4.

Wang, Xiang-Yu, Hao-Ning He, et al. (Apr. 2010). "Klein-Nishina Effects on the High-energy Afterglow Emission of Gamma-ray Bursts". In: *ApJ.* 712.2, pp. 1232–1240. DOI: 10.1088/0004-637X/712/2/1232. arXiv: 0911.4189 [astro-ph.HE].

Wang, Xiang-Yu, Ruo-Yu Liu, et al. (Oct. 2019). "Synchrotron Self-Compton Emission from External Shocks as the Origin of the Sub-TeV Emission in GRB 180720B and GRB 190114C". In: *The Astrophysical Journal* 884.2, 117, p. 117. DOI: 10.3847/1538-4357/ab426c. arXiv: 1905.11312 [astro-ph.HE].

Waxman, Eli (Aug. 1997). "Gamma-Ray–Burst Afterglow: Supporting the Cosmological Fireball Model, Constraining Parameters, and Making Predictions". In: *ApJL.* 485.1, pp. L5–L8. DOI: 10.1086/310809. arXiv: astro-ph/9704116 [astro-ph].

Wu, Qingwen, Bing Zhang, et al. (Jan. 2016). "The extension of variability properties in gamma-ray bursts to blazars". In: *MNRAS.* 455.1, pp. L1–L5. DOI: 10.1093/mnrasl/slv136. arXiv: 1509.04896 [astro-ph.HE].

Wu, Qingwen, Yuan-Chuan Zou, et al. (Sept. 2011). "A uniform correlation between sychrotron luminosity and Doppler factor in Gamma-Ray Bursts and Blazar: A hint of similar intrinsic luminosities?" In: *ApJL.* 740.1,

p. L21. DOI: 10.1088/2041-8205/740/1/L21. URL: https://dx.doi.org/10.1088/2041-8205/740/1/L21.

Xiao, H., S. Krucker, and R. Daniel (Jan. 2022). "GRB221009A/Swift J1913.1+1946: Solar Orbiter STIX measurements." In: *GRB Coordinates Network* 32661, p. 1.

Zdziarski, Andrzej A. and Markus Böttcher (Apr. 2015). "Hadronic models of blazars require a change of the accretion paradigm". In: *MNRASL.* 450.1, pp. L21–L25. ISSN: 1745-3925. DOI: 10.1093/mnrasl/slv039. eprint: https://academic.oup.com/mnrasl/article-pdf/450/1/L21/3084427/slv039.pdf. URL: https://doi.org/10.1093/mnrasl/slv039.

Zhang, Bing and Peter Mészáros (Sept. 2001). "High-Energy Spectral Components in Gamma-Ray Burst Afterglows". In: *ApJ.* 559.1, pp. 110–122. DOI: 10.1086/322400. arXiv: astro-ph/0103229 [astro-ph].

Zhao, Zhi-Chao, Yong Zhou, and Sai Wang (Jan. 2023). "Multi-TeV photons from GRB 221009A: uncertainty of optical depth considered". In: *Eur. Phys. J. C.* 83.1, p. 92. DOI: 10.1140/epjc/s10052-023-11246-y. arXiv: 2210.10778 [astro-ph.HE].